Title

Summary of Laboratory Tests to Assess Mechanical Properties of Permeable Pavement Materials

Authors

Jones, David
Harvey, John T.
Li, H.
et al.

Publication Date

2010-11-01

ITS UCDAVIS
INSTITUTE OF TRANSPORTATION STUDIES

Research Report – UCD-ITS-RR-09-65

Summary of Laboratory Tests to Assess Mechanical Properties of Permeable Pavement Materials

November 2010

David Jones
John T. Harvey
H. Li
Mary M. Campbell

Institute of Transportation Studies ◦ University of California, Davis
1605 Tilia Street ◦ Davis, California 95616
PHONE (530) 752-6548 ◦ FAX (530) 752-6572
www.its.ucdavis.edu

SUMMARY OF LABORATORY TESTS TO ASSESS MECHANICAL PROPERTIES OF PERMEABLE PAVEMENT MATERIALS

TECHNICAL MEMORANDUM

CALTRANS DOCUMENT NO.: CTSW-TM-10-249.01
UCPRC DOCUMENT NO.: UCPRC-TM-2009-05

November 30, 2010

California Department of Transportation

Division of Environmental Analysis

Storm Water Program

1120 N Street, Sacramento, California 95814

http://www.dot.ca.gov/hq/env/stormwater/index.htm

1. Report No.	2. Type of Report	3. Report Phase and Edition
CTSW-TM-10-249.01	Technical Memo	Final

4. Title and Subtitle	5. Report Date
Summary of Laboratory Tests to Assess Mechanical Properties of Permeable Pavement Materials	November 30, 2010
6. Author(s) D. Jones, J. Harvey, H. Li and B. Campbell	**7. Caltrans Project Coordinator** Bhaskar Joshi
8. Performing Organization Names and Addresses Department of Civil and Environmental Engineering One Shields Avenue, EUIII University of California Davis, CA 95616 UC Davis Report Number: UCPRC-TM-2009-05	**9. RTA No.** 249 Amendment No. **10. Contract No.** 43A0249
11. Sponsoring Agency Name and Address California Department of Transportation Division of Environmental Analysis, Storm Water Program 1120 N Street Sacramento, California 95814	**12. Caltrans Functional Reviewers** Bhaskar Joshi, DEA Caltrans
13. Supplementary Notes Project conducted in cooperation with Department of Civil and Environmental Engineering at UC Davis	**14. External Reviewers** DingXin Cheng, California State University, Chico

15. Abstract
This technical memorandum presents a summary of the methods and results related to an assessment of the mechanical properties of fully permeable pavements. The results presented in this tech memo will be used to prepare preliminary pavement designs for fully permeable pavement pilot studies in California and to identify under what conditions they are appropriate to use. The preliminary pavement designs will be presented in a separate technical memorandum.

16. Key Words	17. Distribution Statement	18. No. of pages
Concrete, asphalt, fully permeable pavement, performance test, compaction.		85

For individuals with sensory disabilities, this document is available in alternate formats upon request.

Please call or write to:

Stormwater Liaison,
Caltrans Division of Environmental Analysis, MS 27,
P.O. Box 942874,
Sacramento, CA 94274-0001,

(916) 653-8896 Voice, or dial 711 to use a relay service.

DISCLAIMER

The contents of this technical memorandum reflect the views of the authors who are responsible for the facts and accuracy of the data presented herein. The contents do not necessarily reflect the official views or policies of the State of California or the Federal Highway Administration. This report does not constitute a standard, guideline, specification, or regulation.

This document is not intended to be used as a guideline for the design, construction and maintenance of fully permeable pavements.

PROJECT OBJECTIVES

The objective of this project, titled "Laboratory Testing and Modeling for Structural Performance of Permeable Pavements under Heavy Traffic," is to develop preliminary designs for fully permeable pavements in California.

This objective will be met after completion of five tasks:

1. Evaluate the structural performance characteristics of all the materials potentially used in permeable pavement designs, namely porous asphalt, concrete, base, and subgrade materials.
2. Perform detailed performance modeling of these various designs based upon (1).
3. Develop recommended designs for subsequent accelerated pavement testing and field test sections on the UC Davis campus which are reasonably likely to perform satisfactorily, are constructible, and within reason, economical.
4. Based upon these designs, perform a preliminary life-cycle cost analysis (LCCA) and life-cycle analysis (LCA) of the various options.
5. Compile all the information gathered in this study into a comprehensive final report.

This technical memorandum summarizes the work completed in Task 1.

The objectives did **not** include the preparation of guidelines for the design, construction and maintenance of fully permeable pavements, or any research into the influence of the design of fully permeable pavements on water quality.

TABLE OF CONTENTS

LIST OF TABLES

LIST OF FIGURES

LIST OF TEST METHODS AND SPECIFICATIONS

AASHTO T-11	Standard Method of Test for Materials Finer Than 75-µm (No. 200) Sieve in Mineral Aggregates by Washing
AASHTO T-27	Standard Method of Test for Sieve Analysis of Fine and Coarse Aggregates
AASHTO T-89	Standard Method of Test for Determining the Liquid Limit of Soils
AASHTO T-90	Standard Method of Test for Determining the Plastic Limit and Plasticity Index of Soils
AASHTO T-99	Standard Method of Test for Moisture-Density Relations of Soils Using a 2.5-kg (5.5-lb) Rammer and a 305-mm (12-in.) Drop
AASHTO T-166	Standard Method of Test for Bulk Specific Gravity of Compacted Hot Mix Asphalt (HMA) Using Saturated Surface-Dry Specimens
AASHTO T-198	Standard Method of Test for Splitting Tensile Strength of Cylindrical Concrete Specimens
AASHTO T-209	Standard Method of Test for Theoretical Maximum Specific Gravity and Density of Hot Mix Asphalt (HMA)
AASHTO T-215	Standard Method of Test for Permeability of Granular Soils (Constant Head)
AASHTO T-245	Standard Method of Test for Resistance to Plastic Flow of Bituminous Mixtures Using Marshall Apparatus
AASHTO T-269	Standard Method of Test for Percent Air Voids in Compacted Dense and Open Asphalt Mixtures
AASHTO T-307	Standard Method of Test for Determining the Resilient Modulus of Soils and Aggregate Materials
AASHTO T-320	Standard Method of Test for Determining the Permanent Shear Strain and Stiffness of Asphalt Mixtures using the Superpave Shear Tester
AASHTO T-321	Standard Method of Test for Determining the Fatigue Life of Compacted Hot-Mix Asphalt (HMA) Subjected to Repeated Flexural Bending
AASHTO T-324	Standard Method of Test for Hamburg Wheel-Track Testing of Compacted Hot-Mix Asphalt (HMA)
AASHTO T-331	Standard Method of Test for Bulk Specific Gravity and Density of Compacted Hot-mix Asphalt (HMA) using Automatic Vacuum Sealing Method
AASHTO T-336	Standard Method of Test for Coefficient of Thermal Expansion of Hydraulic Cement Concrete
ASTM PS 129	Standard Provisional Test Method for Measurement of Permeability of Bituminous Paving Mixtures Using a Flexible Wall Permeameter
ASTM C-31	Standard Practice for Making and Curing Concrete Test Specimens in the Field
ASTM C-39	Standard Test Method for Compressive Strength of Cylindrical Concrete Specimens
ASTM C-78	Standard Test Method for Flexural Strength of Concrete (Using Simple Beam with Third-Point Loading)
ASTM D 7064	Standard Practice for Open-Graded Friction Course (OGFC) Mix Design
CT-216	Method of Test for Relative Compaction of Untreated and Treated Soils and Aggregates

Chapter 1. Focus of the Tech Memo

The California Department of Transportation (Caltrans) initiated a controlled laboratory investigation under Master Agreement 65A0108 to evaluate the structural performance of permeable pavements under heavy traffic. The main purpose of this technical memorandum is to present the results of laboratory testing on subgrade, base, and asphalt and portland cement concrete surfacings, which will be used to develop preliminary pavement designs for fully permeable pavement pilot studies and identify conditions if and under which fully permeable pavements can be used on Caltrans highways and facilities.

This technical memorandum is organized as follows:

1. Introduction to the study
2. Experimental design
3. Results of tests on subgrade materials
4. Results of tests on base course materials
5. Results of tests on portland cement concrete wearing course materials
6. Results of tests on asphalt concrete wearing course materials
7. Conclusions

Chapter 2. Introduction

2.1 Problem Statement

Fully permeable pavements are defined for the purposes of this study as those in which all layers are intended to be permeable and the pavement structure serves as a reservoir to store water during storm periods in order to minimize the adverse effects of stormwater runoff. The California Department of Transportation (Caltrans) is interested in investigating the viability and risks of fully permeable pavement designs for use in areas that carry heavy truck traffic as a potential stormwater management best management practice (BMP).

Since the late 1970s, a variety of fully permeable pavement projects have been constructed in a number of U.S. states for low traffic areas and light vehicles. Most of the information available in the literature is about successes, while few failures have been reported for these applications. Observations of several projects by the authors indicate that failures have occurred in localized areas due to clogging of the permeable surface, and to construction processes that have resulted in severe raveling (loss of particles from the surface) or cracking.

As noted, most applications of fully permeable pavements in North America have been for pavements that are not subjected to high-speed traffic or truck traffic, such as parking lots, which reflects road owner concerns about durability. Structural design methods have been empirical in nature, with little or no long-term monitoring data to support the empiricism. Purely empirical design methods require good comprehensive empirical data for all of the expected design conditions, which has limited the speed of technology development for fully permeable pavements because of the high cost of learning from inevitable failures. For this reason it is difficult for purely empirical design methods to consider different materials, climates, subgrades, and structural cross sections because of the need for a large factorial set of performance data that considers all of these design variable permutations. A review of design practice across the United States *(1)* shows the very limited scope of current applications for fully permeable pavements, even by the leading design firms specializing in this type of design. The limited scope of current applications is also reflected in the recently produced National Asphalt Pavement Association (NAPA) *(2)*, American Concrete Pavement Association *(3)*, and Interlocking Concrete Pavement Institute *(4)* manuals for design of porous asphalt, pervious concrete pavements, and permeable interlocking concrete pavements, respectively.

The mechanistic-empirical approach used in this project for the development of new fully permeable pavement designs will increase the speed of technology development. The mechanistic-empirical design development process consists of determining relevant material properties in the laboratory, and then using them in inexpensive and risk-free computer models to evaluate pavement performance, followed by empirical validation and calibration of failure mechanisms and performance of the most promising designs through accelerated pavement testing and field test sections.

There is limited published data on life-cycle cost analysis (LCCA) of fully permeable pavements that include actual costs and performance, and also little information regarding environmental life-cycle assessments (LCA) of fully permeable pavements. There have been several analyses of comparative initial costs for fully permeable pavements compared with conventional pavements, which indicate that the cost of constructing fully permeable pavements is greater than the cost of conventional pavements for residential streets; however some studies indicate that the total initial costs are similar or less because the fully permeable pavements do not require stormwater drainage systems. All of the studies in the literature are for slow-speed facilities with few trucks, and compare different fully permeable pavement systems with different conventional pavements for different applications (streets, parking lots, and other paved areas). None of the studies considered shoulder retrofit of a highway.

2.2 Overall Project Objectives

The study discussed in this report is part of a larger development program being undertaken by the University of California Pavement Research Center (UCPRC) for Caltrans with the objective of developing guidelines, and inputs for specification language, for the use of fully permeable pavements as a potential BMP for controlling stormwater runoff from highways, maintenance yards, rest stops, and other pavements that Caltrans owns and manages.

This objective will be met after completion of laboratory testing to characterize the mechanical and hydrological properties of fully permeable pavement materials, structural and hydrological performance modeling to develop initial designs, life-cycle cost analyses and environmental life-cycle assessment studies, and full-scale testing in the field and/or using accelerated pavement testing (using the Caltrans Heavy Vehicle Simulator [HVS]) to validate the structural and hydrological designs, or if necessary to calibrate them to match the observed field performance. This step-wise development process of first performing laboratory testing and computer modeling, followed by full-scale validation with the HVS and field test sections is the typical process being used for development of other pavement technologies for

Caltrans. Caltrans pavement designers have been involved in the process of reviewing the results of this development process, and the planning for this current project. As with any other new pavement technology, there is no commitment by Caltrans to implement it until the development process has reached a point at which the uncertainties have been sufficiently addressed to reduce the risk of pilot section failure on the state highway network to an acceptable level.

Successful completion of this project will provide Caltrans with structural design procedures, performance estimates, life-cycle cost analyses, and an environmental life-cycle assessment framework to compare fully permeable pavement BMPs with existing approved BMPs.

2.3 Objectives for this Phase of the Study

The goal of the project covered in this current task order (RTA249), entitled *Laboratory Testing and Modeling for Structural Performance of Permeable Pavements under Heavy Traffic* is to develop preliminary fully permeable pavement designs that can be tested in pilot studies under typical California traffic and environmental conditions *(5)*. This goal will be achieved on completion of the following tasks:

1. Review the latest literature.
2. Prepare and test specimens in the laboratory for the structural properties necessary for undertaking a mechanistic-empirical design of fully permeable pavement structures. Develop new testing methods if required to evaluate non-traditional materials. Include the materials testing properties in the Mechanistic-Empirical Pavement Design materials database developed by the University of California Pavement Research Center (UCPRC) for Caltrans.
3. Prepare additional specimens for hydraulic performance testing in the laboratory as part of the companion task order (RTA247, *Laboratory Testing and Modeling for Hydraulic Performance of Permeable Pavements under Heavy Traffic*).
4. Estimate pavement performance for prototype designs using the laboratory test results in pavement performance models.
5. Perform a preliminary life-cycle cost analysis and environmental life-cycle assessment of the various options.
6. Based on the results of the computer model analysis, develop detailed structural designs for HVS and field test sections that include pavement dimensions and material specifications.

This report covers Task 2.

The results of this development process are essential inputs to life-cycle cost analysis (LCCA) and life-cycle analysis (LCA). Preliminary LCCA and LCA will be performed towards the end of this study based on the results of the refined designs. Results will be presented in a separate document. More detailed life-cycle cost analysis (LCCA) and life-cycle assessment (LCA) will need to be performed after construction, evaluation, and performance validation of accelerated pavement test sections and field test

sections to provide more realistic initial cost information and improved maintenance and rehabilitation cost estimates.

Chapter 3. Experimental Design

The approach used for development of detailed pavement designs in this study is referred to as "mechanistic-empirical" or "ME". Caltrans is in the process of implementing this approach as a replacement for the empirical R-value design method. The assumptions of R-values designs (levels of compaction, pavement structural layering, etc) are also not appropriate for permeable pavements. The ME approach will be used for both flexible and rigid permeable pavements to produce a set of designs for different Traffic Indexes (TI), climate and soil conditions, similar to the catalog designs prepared by the UCPRC for the Caltrans Rigid Pavement Design Catalog currently used in the Caltrans Highway Design Manual (HDM).

The structural properties of interest include stiffness, strength, durability, fatigue performance, and rutting performance. The proposed *(5)* and actual testing plans followed in the laboratory testing study are shown in Table 3.1 through Table 3.5. Differences between the proposed and actual test plans are discussed below.

3.1 Subgrade Materials

Initial studies of the properties of clays in California revealed that there is little difference in the strength and permeability characteristics of these materials. Consequently, only one clay and one silt material were tested, instead of two clays and one silt as proposed. The testing of a CH clay was considered unnecessary given the known poor bearing capacity and permeability characteristics of these materials, and the unlikelihood that a fully permeable pavement would be constructed on this type of material. An analysis of early results on the silt and clay materials indicated that results were sensitive to changes in moisture content. Consequently, additional tests were carried out on the two materials to assess a broader range of moisture contents (and densities on the clay) instead of testing the second clay.

Sand and gravel subgrades were not included because they are expected to perform well in terms of both structural capacity and permeability, and are not as sensitive to the saturation levels expected in permeable pavements in California.

Table 3.1: Summary of Test Plan for Subgrade Materials and Permeable Gravel Base

Layer	Properties of Interest	Test Type	Materials	Compaction (%)	Saturation	Gradation	Moisture Content	Replicate	Total Tests[1]
Proposed Test Plan									
Subgrade	Stiffness	AASHTO-T307[2]	1 x Silt, 2 x Clays	80, 90	Saturated, Unsaturated	As excavated	OMC[4], OMC -2%	1	24
	Rutting resistance	TRLT[3]	1 x Silt, 2 x Clays	80, 90	Saturated, Unsaturated	As excavated	OMC, OMC -2%	1	24
Base	Stiffness	AASHTO-T307	1 x Crushed gravel 1 x Recycled concrete 1 x Recycled glass 1 x Recycled tire blend	n/a	Saturated, Unsaturated	3	n/a	1	24
Actual Test Plan									
Subgrade	Stiffness	AASHTO-T307	1 x Silt 1 x Clay	90, 95 80, 85, 90, 95	Saturated Unsaturated	As excavated	OMC, OMC -2%, OMC +3% OMC, OMC -2%, OMC + 3%, +8%	1	44
	Rutting resistance	TRLT	1 x Silt 1 x Clay	80, 90	Saturated Unsaturated	As excavated	OMC, OMC -2%, OMC +3% OMC, OMC -2%, OMC + 3%, +8%	1	28
Base	Stiffness Permeability	AASHTO-T307	3 x Crushed gravel	n/a	Saturated Unsaturated	As supplied	n/a	2	12

[1] Total tests = Compaction x Saturation x Gradations x Moisture Contents x Materials x Test Variables.
[2] Triaxial Stiffness Test. [3] Triaxial Repeated Load Test. [4] Optimum moisture content.

Table 3.2 Summary of Test Plan for Permeable Concrete Subbase

Layer	Properties of Interest	Test Type	Materials	Air-voids (%)	Gradations	Test Variables	Total Tests[1]
Proposed Test Plan							
Surface	Compressive strength	ASTM C-35[2]	1 x Recycled concrete	20 25	3	3 replicates	18
	Fatigue resistance	ASTM C-78[3]	1 x Recycled concrete	20 25	3	3 replicates	18
	Flexural strength	ASTM C-78[4]	1 x Recycled concrete	20 25	3	3 replicates	18
Actual Test Plan							
Subbase	Compressive strength	ASTM C-35	1 x Crushed Gravel	n/a[5]	6	3 replicates	18

[1] Total tests = Materials x Air-Voids x Gradations x Test Variables.
[2] Compressive Strength Test. [3] Flexural Controlled-Deformation Fatigue Test. [4] Flexural Beam Test.
[5] Air-void content is dependent on gradation.

Table 3.3: Summary of Test Plan for Permeable Concrete Wearing Course

Layer	Properties of Interest	Test Type	Materials	Air-voids (%)	Gradations	Cement Content	Test Variables	Total Tests
Proposed Test Plan								
PCC Wearing Course	Compressive strength	ASTM C-35	1 x Crushed aggregate	15 20	3	1	3 replicates	18
	Fatigue resistance	ASTM C-78	1 x Crushed aggregate	15 20	3	1	3 replicates	18
	Flexural strength	ASTM C-78	1 x Crushed aggregate	15 20	3	1	3 replicates	18
	Coefficient of thermal expansion	AASHTO T-336	2 x Crushed aggregate	15 20	3	1	2 replicates	24
Actual Test Plan								
PCC Wearing Course	**Phase 1**							
	Permeability	ASTM PS 129	1 x Crushed aggregate	n/a[1]	6	1	3 replicates	18
	Compressive strength		1 x Crushed aggregate	n/a	6	1	5 replicates	30
	Phase 2							
	Permeability	ASTM PS 129	1 x Crushed aggregate	n/a	3	1	3 replicates	9
	Compressive strength	ASTM C-35	1 x Crushed aggregate	n/a	3	1	3 replicates	9
	Split tensile strength	ASTM T-198	1 x Crushed aggregate	n/a	3	1	5 replicates	15
	Flexural strength	ASTM C-78	1 x Crushed aggregate	n/a	3	1	3 replicates	15
	Fatigue resistance	ASTM C-78	1 x Crushed aggregate	n/a	3	1	3 replicates	9
	Phase 3							
	Permeability	ASTM PS 129	3 x Crushed aggregate	n/a	3	2	3 replicates	9
	Compressive strength	ASTM C-78	3 x Crushed aggregate	n/a	3	2	3 replicates	9
	Split tensile strength	ASTM T-198	3 x Crushed aggregate	n/a	3	2	5 replicates	9
	Coefficient of thermal expansion	AASHTO T-336	2 x Crushed aggregate	n/a	3		2 replicates	24

[1] Air-void content is dependent on gradation.

Table 3.4: Summary of Test Plan for Precast/Cast In-Place Concrete Wearing Course

Layer	Properties of Interest	Test Type	Materials	Hole Types	Hole Configurations	Gradations	Test Variables	Total Tests[1]
Proposed Test Plan								
PCC Wearing Course	Fatigue resistance	ASTM C-78[2]	1 x Crushed aggregate	2	4	1	3 replicates	24
	Flexural strength	ASTM C-78[3]	1 x Crushed aggregate	2	10	1	2 replicates	40
Actual Test Plan								
PCC Wearing Course	Permeability	ASTM PS 129	1 x Crushed aggregate	1	1	1	3 replicates	3
	Fatigue resistance	ASTM C-78	1 x Crushed aggregate	1	1	1	3 replicates	3
	Flexural strength	ASTM C-78	1 x Crushed aggregate	1	1	1	2 replicates	2

[1] Total tests = Hole Types x Hole Configurations x Gradations x Test Variables.
[2] Flexural Controlled-Deformation Fatigue Test.
[3] Flexural Beam Test.

Table 3.5: Summary of Test Plan for Permeable Asphalt Wearing Course

Layer	Properties of Interest	Test Type	Materials	Mixes	Air-voids (%)	Gradations	Test Variables	Total Tests
Proposed Test Plan								
Asphalt Wearing Course	Stiffness	AASHTO T-321[1]	1 x Crushed aggregate	1 x HMA-O 1 x R-HMA-O	15 20	2	3 x temperatures 1 x strain level 1 x replicates	24
	Fatigue resistance	AASHTO T-321[2]	1 x Crushed aggregate	1 x HMA-O 1 x R-HMA-O	15 20	2	1 x temperatures 2 x strain level 2 x replicates	32
	Rutting resistance	AASHTO T-324[3]	1 x Crushed aggregate	1 x HMA-O 1 x R-HMA-O	15 20	2	1 x temperatures 2 x strain level 2 x replicates	48
	Moisture sensitivity							
Actual Test Plan								
Asphalt Wearing Course	Permeability	ASTM PS 129	3 x Crushed aggregate	17[4]	n/a[5]	n/a[5]	3 x replicates	51
	Flexural Stiffness	AASHTO T-321[1]	3 x Crushed aggregate	17	n/a	n/a	3 x temperatures 1 x strain level 2 x replicates	102
	Fatigue resistance	AASHTO T-321[2]	4 x Crushed aggregate	4	n/a	n/a	1 x temperature 2 x strain levels 3 x replicates	24
	Rutting resistance	AASHTO T-320[6]	3 x Crushed aggregate	17	n/a	n/a	1 x temperatures 1 x stress level 3 x replicates	51
	Moisture sensitivity	AASHTO T-324[3]	3 x Crushed aggregate	17	n/a	n/a	3 x replicates	51
	Raveling resistance	ASTM D7064[7]	3 x Crushed aggregate	17	n/a	n/a	3 x conditions 3 x replicates	153

1 Flexural Frequency Sweep Test.
2 Flexural Controlled-Deformation Fatigue Test.
3 Hamburg Wheel Track Test.
4 Includes a range of aggregate sizes, sources, binder types, and fillers.
5 Air-voids dependent on gradation.
6 Repeated simple shear test.
7 Standard Practice for Open-Graded Friction Course (OGFC) Mix Design (Cantabro Test).

3.2 Granular Base Materials

The proposed experimental design considered an assessment of one crushed gravel and three different waste materials, namely, crushed concrete, crushed glass, and an aggregate/recycled tire blend. Discussions with the California Department of Resources Recycling and Recovery and various aggregate suppliers revealed the following:

- Concrete construction waste is generally crushed into aggregate base material. The costs of producing an open grade material suitable for fully permeable base and dealing with the excess finer material were considered to be high and it is unlikely that producers would be willing to produce this type of material in the quantities that would be required for constructing/retrofitting fully permeable pavements or pavement shoulders.
- Most waste glass is recycled for use in new glass products and the remainder is currently used in landscaping projects. Its use as a base course material in fully permeable pavements would have a significantly lower value compared to its reuse in glass products and no producers were willing or able to provide samples for assessment.
- Current waste tire processing techniques do not produce an appropriately sized/shaped particle for use in a fully permeable pavement layer.

Consequently, the testing of fully permeable base course materials focused on three commercially available aggregates in the state with different geological origins. Performance of these materials was then compared with the results obtained by other researchers elsewhere in the United States. The aggregate gradations included in the study use smaller stone than is currently recommended by the National Asphalt Paving Association's (NAPA) and the American Concrete Pavement Association's (ACPA) permeable pavement guidelines. Discussions with three northern California aggregate producers revealed that the larger stone gradations (approximately 1.5 in to 2.0 in [38 mm to 50 mm] maximum aggregate size) in the guidelines are generally not commercially available or are much more expensive to produce than products with a maximum aggregate size of approximately ¾ in to 1.0 in (19 mm to 25 mm).

3.3 Permeable Concrete Subbase

This phase of testing was done in parallel with the first phase of testing on the permeable concrete wearing course discussed in Section 3.4, given that the only difference in experimental design was the air-void content of the mix. Fatigue resistance and flexural strength testing were also omitted from this part of the study, since a review of the literature, and research team experience from previous studies on "inverted" pavements (where a cemented subbase is used to provide a platform for compaction and confinement of the base, as well as to provide structural integrity in the lower layers of the pavement) indicated that cracks in this lower pavement layer would not significantly influence the pavement

performance, and would in fact improve the flow of water through the structure. Only crushed gravel materials were used, due to the problems in obtaining recycled concrete described in the previous section.

3.4 Permeable Concrete Wearing Course

A literature review of available published information revealed very little useful information on the optimization of aggregate gradings and cement contents for permeable concrete wearing course applications. The actual testing program therefore differed from the planned program in that a phased approach was followed, starting with preliminary testing (Phase 1) on a broad range of gradings identified in the literature. Compressive strength and permeability tests were carried out on specimens prepared in this phase to identify the best balance between these two attributes. This was followed by more comprehensive testing (Phase 2) on specimens prepared with the three most promising gradings identified in Phase 1. Additional testing (Phase 3) was then carried out to assess the effects of a number of other parameters including cement content, water-cement ratio, and particle shape. A final phase of testing (Phase 4) to compare open-graded mixes with slabs with pre-cast/cast in place drainage holes was also undertaken (discussed in Section 3.5).

3.5 Precast/Cast In-Place Concrete Wearing Course

Testing plans in this phase of the study were changed due to the difficulty in producing small scale specimens with appropriate hole sizes and hole distributions to replicate full-scale situations. Only one design was ultimately used, which simulated a pre-cast slab containing 10 mm diameter holes at a pre-calculated spacing that would drain the calculated water flows from the pavement, whilst also providing a wearing course suitable for bicycle, motorcycle and motor vehicle traffic. Attempts to produce laboratory-scale precast specimens with slots instead of holes and to produce laboratory-scale cast in-place specimens representative of appropriate construction practices in the field were not successful. Instead, it was decided to rather understand the failure behavior of the specimens produced and then to model other possible combinations using a finite element approach.

3.6 Porous Asphalt Wearing Course

Testing plans in this phase were changed to cover a broader range of mix designs and to undertake additional tests to assess issues considered important in the design of open-graded mixes. The testing was linked to another project assessing open-graded friction courses for use in “quiet” pavements, being undertaken by the UCPRC on behalf of the Caltrans Division of Research and Innovation (work was

planned and managed separately for each project to ensure that costs were attributed correctly and that no work was charged for twice). A total of 19 mixes, including a dense-graded control, were assessed. Limited testing was carried out on a European mix, specimens of which were provided to UCPRC from a test track in Spain. These 19 mixes included five different binders (original test plan considered two) and three different aggregates (original test plan considered one). A range of aggregate sizes, gradations, and air-void contents were covered in the mixes. Additional testing included shear tests as a second test to assess rutting performance and a durability test to assess resistance to raveling. Permeability tests were also undertaken on a set of specimens from each mix.

Chapter 4. Subgrade Materials

4.1 Introduction

Subgrade materials are generally the in situ soils below a pavement structure. On existing pavements, they are usually compacted as densely as possible to provide a platform for the overlying pavement layers and to provide added structural integrity to the pavement. However, on fully permeable pavements, compaction of the subgrade is generally restricted where possible to facilitate infiltration of water. This requires a thicker overlying pavement structure to compensate for the reduced subgrade strength. Testing of subgrade materials focused on the influence of different levels of compaction and different moisture contents on the stiffness of those materials.

4.2 Material Sampling

Clay subgrade material was sampled from an undisturbed area near the UCPRC research facility. The silt material was sampled from an undisturbed area near Stockton. The materials were considered representative of clay and silt materials in California.

4.3 Test Results

4.3.1 Grading Analysis

The grading analysis was carried out following AASHTO Test Method T 11. A hydrometer analysis was not undertaken. The results for the two soils are shown in Figure 4.1. The gradings are typical for these soil types and were considered to provide a good representation of subgrade soils in the Central Valley of California. They should be representative of other areas of the state as well, and provide an adequate variation to understand the behavior in terms of fully permeable pavements.

4.3.2 Atterberg Limits

The Atterberg Limits were determined following AASHTO Test Methods T 89 and T 90. The Atterberg limits for the two soils and their soil classification based on the grading analysis and Atterberg limits are summarized in Table 4.1. The difference between the two soil types was considered sufficient for distinguishing performance trends. Although clays with much higher plasticity indices are common in California, the testing of these clays was not considered necessary as they would typically not be considered suitable for supporting fully permeable pavement structures.

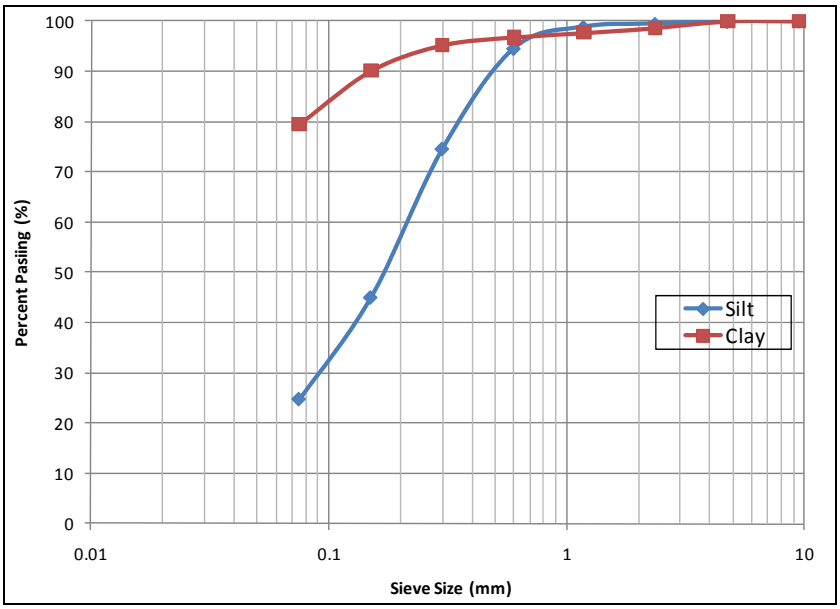

Figure 4.1: Subgrade materials grading analysis

Table 4.1: Subgrade Soil Atterberg Limits

	Atterberg Limits		
Soil Type	**Liquid Limit**	**Plastic Limit**	**Plasticity Index**
Silt	Soil pat slips	Non-plastic	0
Clay	30.9	18.5	12.4
Soil Type	**Classification**		
	USCS[1]	**AASHTO[2]**	
Silt	ML	A-2-4	
Clay	CL	A-6	

[1] USCS – Unified Soil Classification System
[2] AASHTO – American Association of State Highway and Transport Officials

4.3.3 Density-Moisture Relationships

The maximum dry density and optimum moisture content of each material were determined using AASHTO Test Method T 99 (Method A) as well as Caltrans Test Method CT 216. Results are summarized in Table 4.2 and in Figure 4.2 and Figure 4.3.

Table 4.2: Optimum Moisture content and Maximum Density of Silt and Clay

Soil Type	Wet Density[1] (kg/m^3)		Dry Density[1] (kg/m^3)		Optimum Moisture Content (%)	
	AASHTO	Caltrans	AASHTO	Caltrans	AASHTO	Caltrans
Silt	2,070	2,150	1,850	1,920	12	12
Clay	2,100	2,170	1,800	1,910	17	14

[1] Densities rounded to nearest 10 kg/m^3

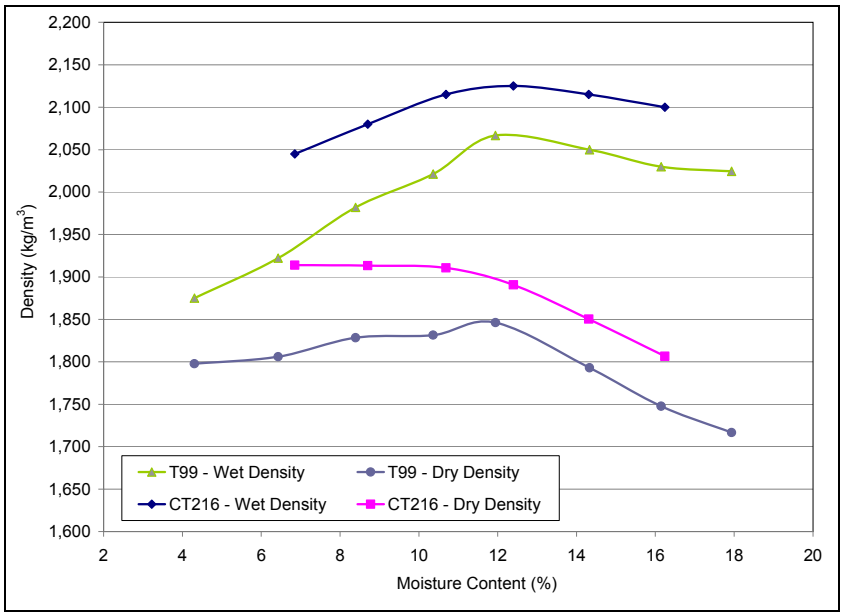

Figure 4.2: Subgrade moisture-density relationships for silt material.

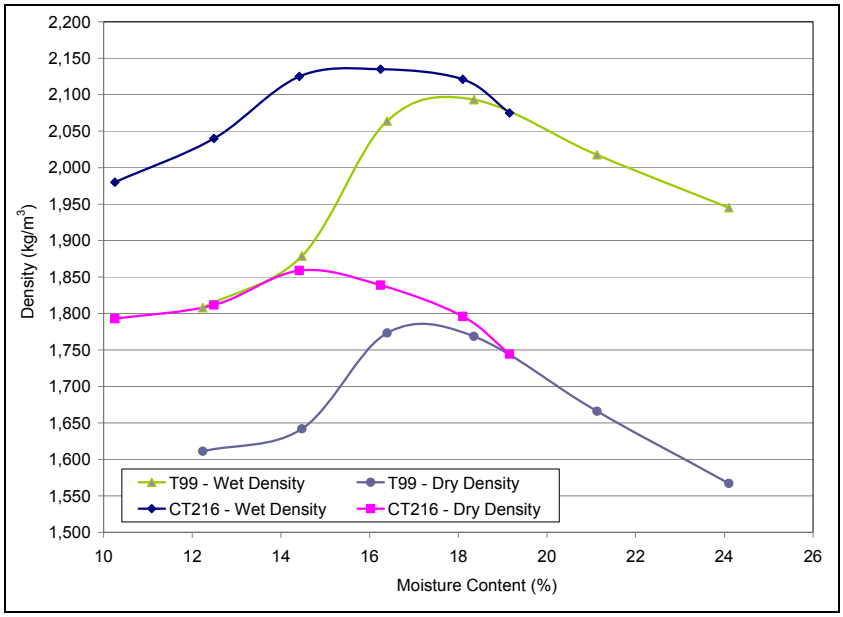

Figure 4.3: Subgrade moisture-density relationship for clay material.

The results show that the densities obtained using the Caltrans method were approximately five percent higher than those determined using the AASHTO method. The optimum moisture contents of the silt material were the same for both test methods, but were significantly different for the clay material (Caltrans method was four percent lower). The differences were attributed to the different compaction energies and amount of shearing in the two methods.

The AASHTO densities and optimum moisture content were selected for all further work as this provided a more conservative representation of field conditions.

4.3.4 Permeability

Permeability of the silt and clay materials for a range of compaction levels was determined using AASHTO Test Method T 215 (constant head method). The results are summarized in Figure 4.4 and Figure 4.5.

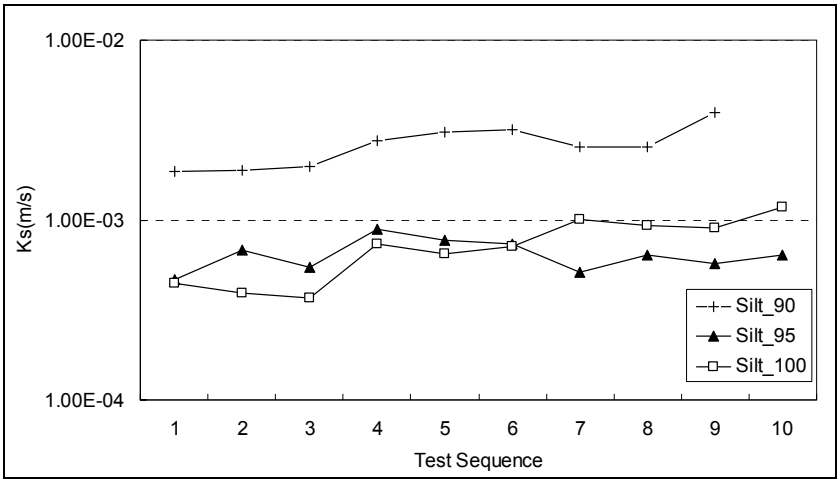

Figure 4.4: Saturated hydraulic conductivity for silt.
(Note permeability determined using AASHTO T-215 [constant head])

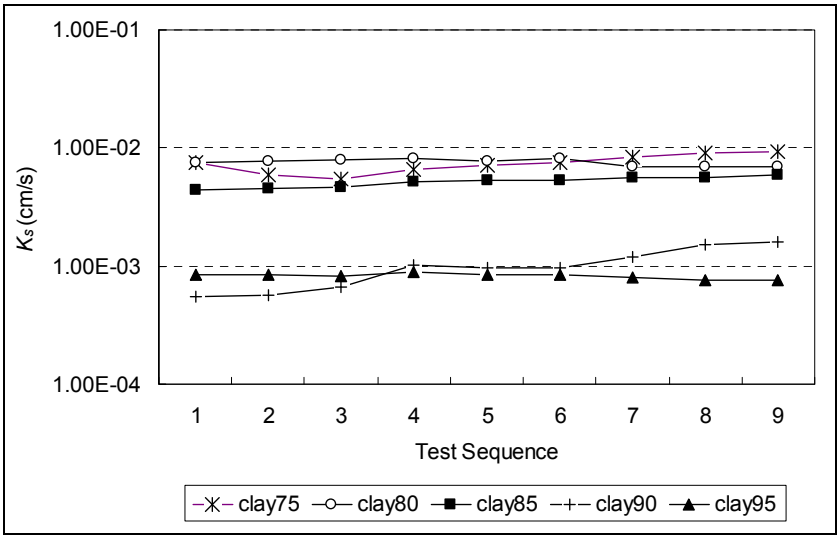

Figure 4.5: Saturated hydraulic conductivity for clay.
(Note permeability determined using AASHTO T-215 [constant head])

Permeability on both materials was poor and decreased with increasing compaction as expected. The clay material was more consistent than the silt, which was attributed to the finer gradation. The relationship between permeability and soil compaction for the silt and clay is shown in Figure 4.6. The reduction in permeability with increasing compaction was not as significant for the silt as it was for the clay. The permeability of the clay decreased from 10^{-2} cm/s (natural, uncompacted in situ soil) to 10^{-5}cm/s (100 percent of laboratory determined maximum dry density) over the range of compactions tested.

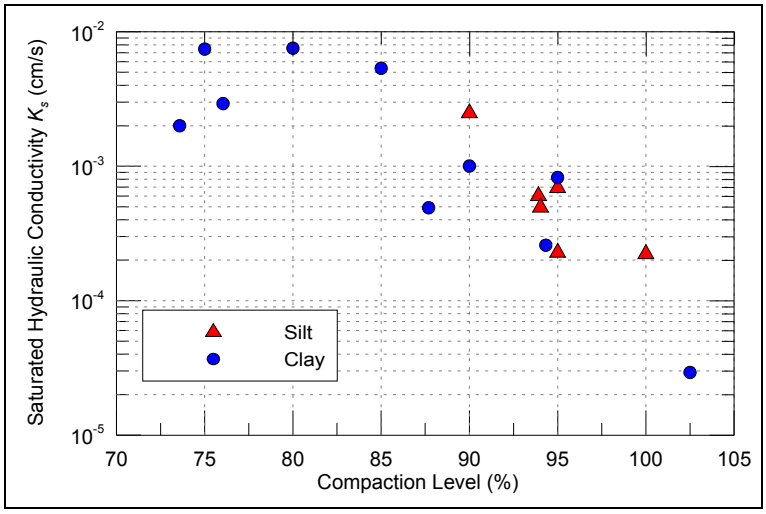

Figure 4.6: Saturated hydraulic conductivity vs. compaction level of silt and clay.
(Note permeability determined using AASHTO T-215 [constant head])

4.3.5 Resilient Modulus

The resilient modulus of each material was assessed using AASHTO Test Method T 307, using the testing sequence summarized in Table 4.3. Specimens were prepared using the moisture content and density determined in Section 4.3.3 as a baseline, with additional specimens prepared with different density and moisture content combinations.

Resilient Modulus of Silt Material

Specimens for determining the resilient modulus of the silt material were prepared as follows:

- Two different density combinations:
  90 and 95 percent of the previously determined AASHTO density. Densities below 90 percent were not considered for tests on the silt material as it is unlikely that such a low density would be found on a highway given the natural compaction of the soil and additional compaction through unavoidable movements of the construction equipment.
- Three different optimum moisture content (OMC) combinations
  OMC, OMC – 2 percent, and OMC + 3 percent. Testing in the saturated condition was not undertaken due to difficulties in preparing specimens (specimens "failed" before testing started)

and the knowledge gained from testing at the three selected moisture contents, which indicated that the soils would have little or no bearing capacity at higher moisture contents.

Table 4.3: Testing Sequence for Resilient Modulus of Subgrade Soil

Sequence No.	Confining Pressure, σ_3		Max. Dev. Stress, σ_d		No. of Load Applications
	kPa	psi	kPa	psi	
0	42	6	28	4	500
1	42	6	14	2	100
2			28	4	
3			42	6	
4			56	8	
5			70	10	
6	28	4	14	2	100
7			28	4	
8			42	6	
9			56	8	
10			70	10	
11	14	2	14	2	100
12			28	4	
13			42	6	
14			56	8	
15			70	10	

The results of the resilient modulus testing on the silt material are summarized in Table 4.4 and in Figure 4.7 through Figure 4.9 and are consistent with results presented in the literature *(6,7)*. It should be noted that preparing and handling stable specimens at the lower densities and higher moisture contents proved difficult and consequently tests on these combinations were not possible.

Figure 4.7 shows that the resilient modulus increased with an increase in confining pressure and decreased with an increase in moisture content, as expected. The relationship between resilient modulus and deviator stress showed similar trends, but was less significant. The specimen with the highest compaction and lowest moisture content had the highest resilient modulus, and the specimen with the lowest compaction and highest moisture content had the lowest resilient moisture content, as expected. The influence of moisture content was more significant than that of compaction level and small changes in moisture are likely to have a significant influence on the strength and stiffness of subgrade materials. It should, however, be noted that under field conditions, saturated soils under pavements still have some strength due to natural confinement of the surrounding soil and compacted layers above.

Table 4.4: Silt: Results of Resilient Modulus Testing

Conf. Pressure (kPa)	Dev. Stress (kPa)	Resilient Modulus (MPa)					
		90% Compaction			95% Compaction		
		MC=10%	MC=12%	MC=15%	MC=10%	MC=12%	MC=15%
14	13	66	57	41	88	71	53
	26	60	52	38	80	65	50
	39	64	56	40	85	70	52
	52	64	53	NR	89	72	54
	65	56	NR	NR	86	66	53
28	13	92	81	56	120	98	66
	26	82	73	50	110	90	60
	39	84	75	52	111	92	63
	52	86	77	53	115	95	64
	65	86	77	54	118	97	65
42	13	116	108	72	148	123	91
	26	111	101	67	142	120	87
	39	110	99	66	142	119	85
	52	106	95	65	140	118	83
	65	105	94	65	139	117	81

MC = Moisture Content NR = No result

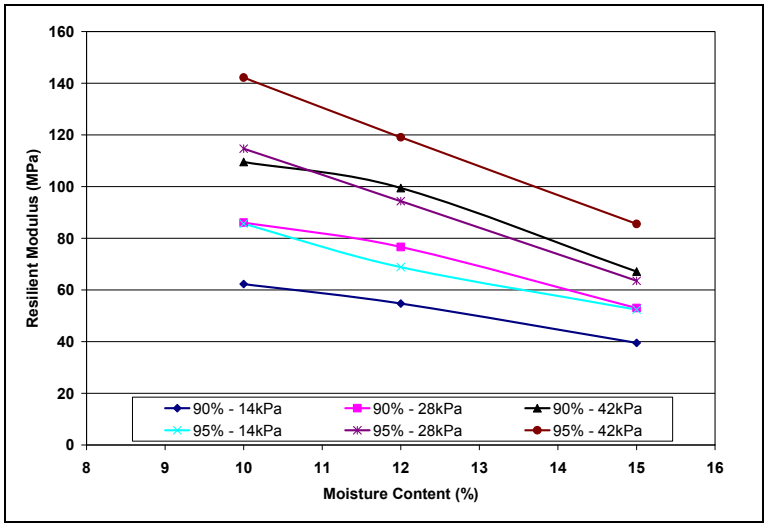

Figure 4.7: Silt: Resilient modulus vs. compaction moisture content for different confining pressure.

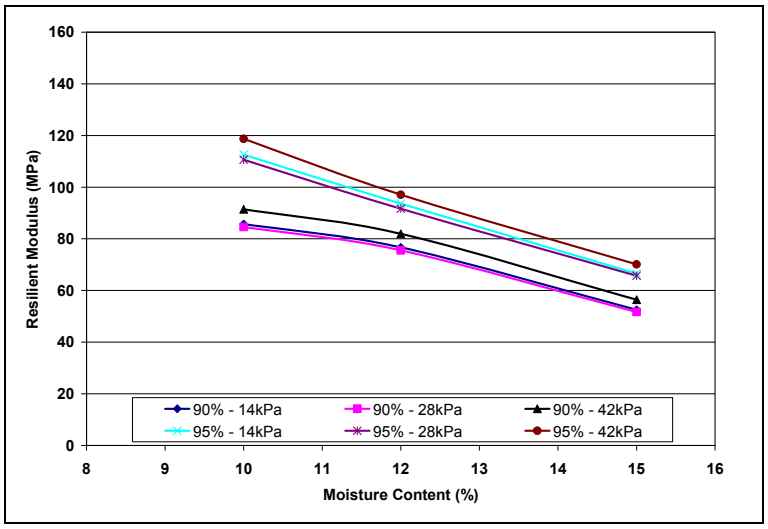

Figure 4.8: Silt: Resilient modulus vs. compaction moisture content for different deviator stresses.

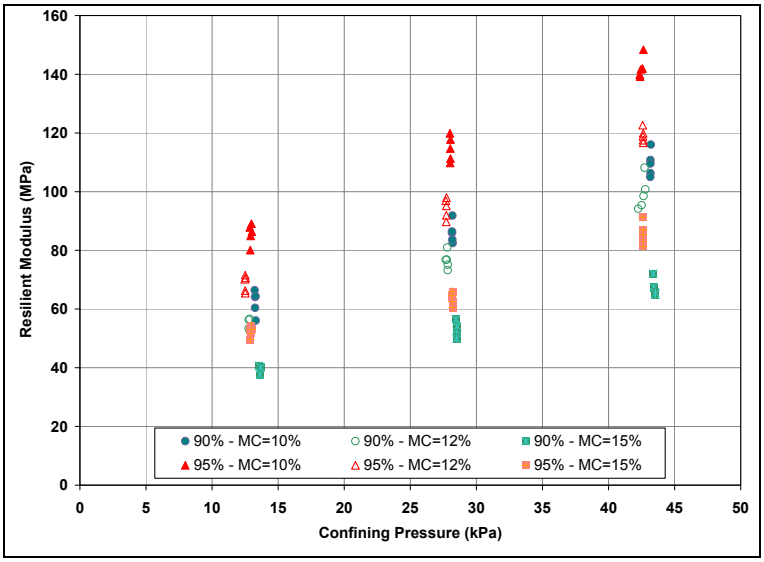

Figure 4.9: Silt: Resilient modulus vs. confining pressure.

Resilient Modulus of Clay Material

Specimens for determining the resilient modulus of the clay material were prepared as follows:

- Four different density combinations:
  80, 85, 90, and 95 percent of the previously determined AASHTO density. Densities below 90 percent were considered for tests on the clay materials. Although it is unlikely that such a low density would be found on a highway given the natural compaction of the soil and additional compaction through unavoidable movements of the construction equipment, possible worst case conditions representing high rainfall events, or prolonged rainfall, at the lower densities were assessed.

- Four different moisture content combinations:
  OMC, OMC – 2 percent, OMC + 3 percent, OMC + 5 percent. Testing under saturated conditions was not undertaken for the same reasons as those provided for the silt material.

The results of the resilient modulus testing on the clay material are summarized in Table 4.5 and in Figure 4.10 through Figure 4.13. It should be noted that preparing stable specimens at the lower densities and higher moisture contents proved difficult and therefore the full range of moisture contents are only shown for the 90 percent compaction level (i.e. most likely field compaction). Figure 4.10 shows the increase in resilient modulus with increasing compaction for a deviator stress of 42 kPa. All figures show that stiffenss increased with higher densities and lower moisture contents, as expected. Small changes in moisture are likely to have a significant influence on the strength and stiffness of clay materials. The influence of moisture content was more significant than that of compaction level.

Table 4.5: Clay: Results of Resilient Modulus Testing

Conf. Pressure (kPa)	Dev. Stress (kPa)	Resilient Modulus (MPa)									
		80% Compaction		85% Compaction		90% Compaction				95% Compaction	
		MC=15%	MC=17%	MC=15%	MC=17%	MC=15%	MC=17%	MC=20%	MC=25%	MC=15%	MC=17%
14	13	105	87	130	103	179	118	101	NR	201	140
	26	87	73	114	88	161	101	87	NR	185	117
	39	79	63	104	78	151	90	78	NR	175	105
	52	71	56	97	70	142	82	73	NR	167	95
	65	66	51	91	65	135	76	68	NR	160	88
28	13	110	95	141	113	192	125	107	NR	215	146
	26	94	77	122	95	171	107	89	NR	194	126
	39	83	66	111	82	157	94	81	NR	183	110
	52	75	58	102	73	147	85	74	NR	172	98
	65	70	53	95	67	139	79	71	NR	164	91
42	13	112	93	141	108	190	128	107	19	217	149
	26	97	79	125	91	171	111	97	13	198	128
	39	85	67	113	81	158	98	89	10	185	112
	52	77	59	103	73	148	87	80	10	173	101
	65	71	53	96	67	139	80	73	NR	163	92

MC = Moisture Content NR = No result

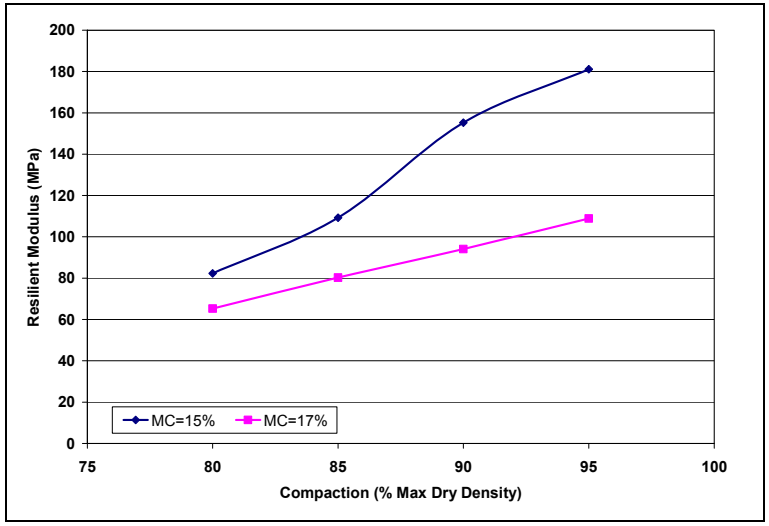

Figure 4.10: Clay: Resilient modulus vs. compaction.

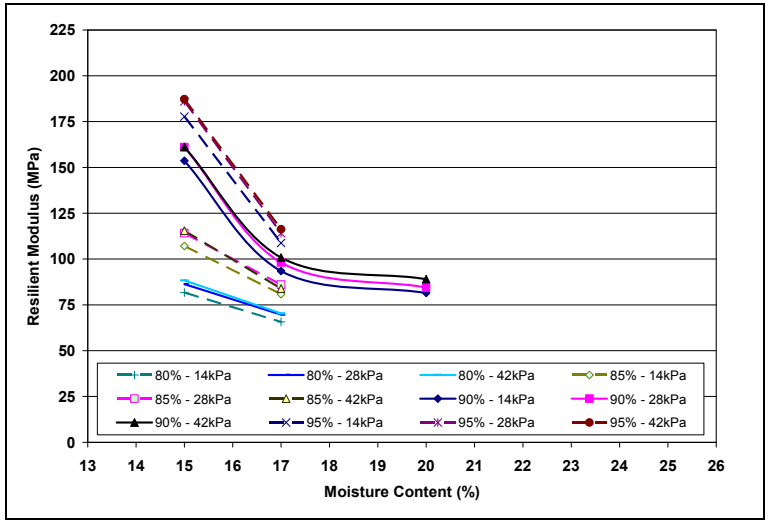

Figure 4.11: Clay: Resilient modulus vs. compaction moisture content for different confining pressure.

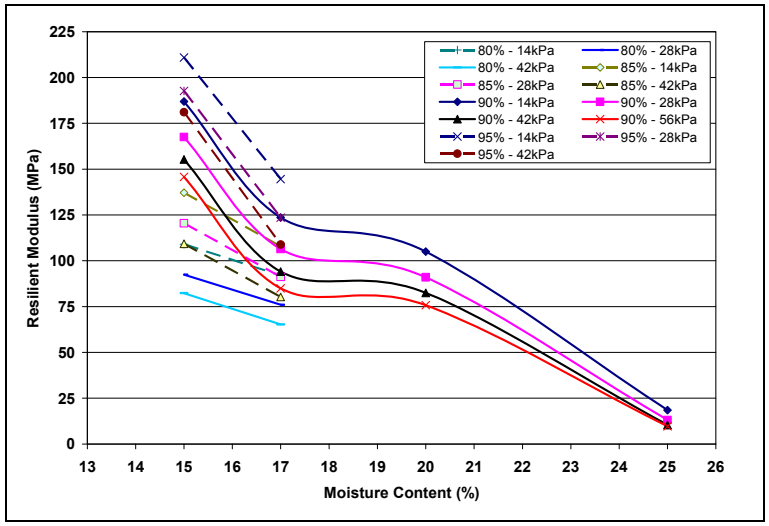

Figure 4.12: Clay: Resilient modulus vs. compaction moisture content for different deviator stresses.

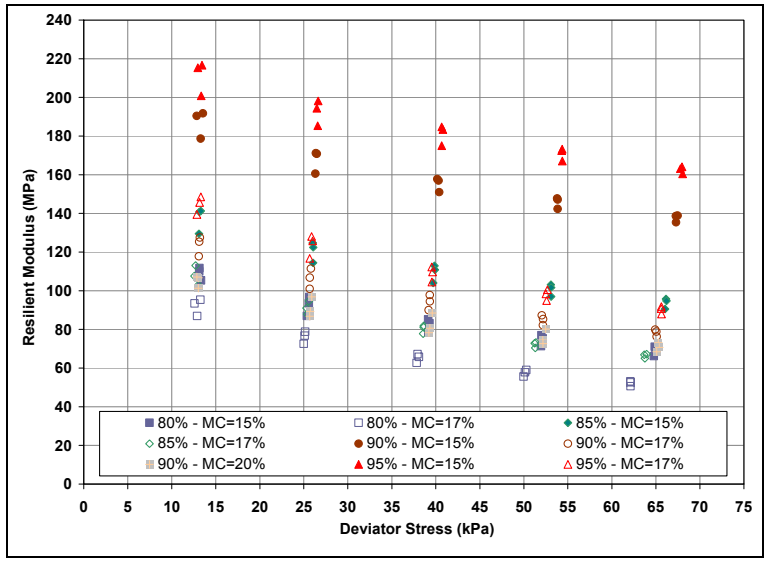

Figure 4.13: Clay: Resilient modulus vs. deviator stress.

4.3.6 Permanent Deformation

Repeated load permanent deformation test specimens were prepared using the moisture contents and densities determined in Section 4.3.3 as a basis. The permanent deformation of each specimen was assessed using the testing sequence summarized in Table 4.6. Lower loads were used on the high moisture content specimens to limit very early failures.

Table 4.6: Testing Sequence of Permanent Deformation for Subgrade Soil

Moisture Content	Sequence No.	Confining Pressure, σ_3		Max. Deviator Stress, σ_d		No. of Load Applications
		kPa	psi	kPa	psi	
Silt						
10%, 12%	1	14	2	28	4	1,000
	2			42	6	2,000
	3			56	8	3,000
	4			70	10	5,000
	5			84	12	9,000
Total						**20,000**
15%	1	14	2	14	2	1,000
	2			28	4	1,000
	3			42	6	2,000
	4			56	8	3,000
	5			70	10	5,000
	6			84	12	9,000
Total						**21,000**
Clay						
15%, 17%	1	14	2	42	6	1,000
	2			70	10	2,000
	3			98	14	3,000
	4			126	18	5,000
	5			154	22	9,000
Total						**20,000**
20%, 25%	1	14	2	21	3	1,000
	2			42	6	1,000
	3			70	10	2,000
	4			98	14	3,000
	5			154	22	5,000
	6			154	22	9,000
Total						**21,000**

The results of the repeated load permanent deformation tests on the silt and clay materials are shown in Figure 4.14 and Figure 4.15 respectively and show that both materials will add very little strength (permanent deformation resistance) to a pavement structure, with performance negatively influenced with increasing moisture content.

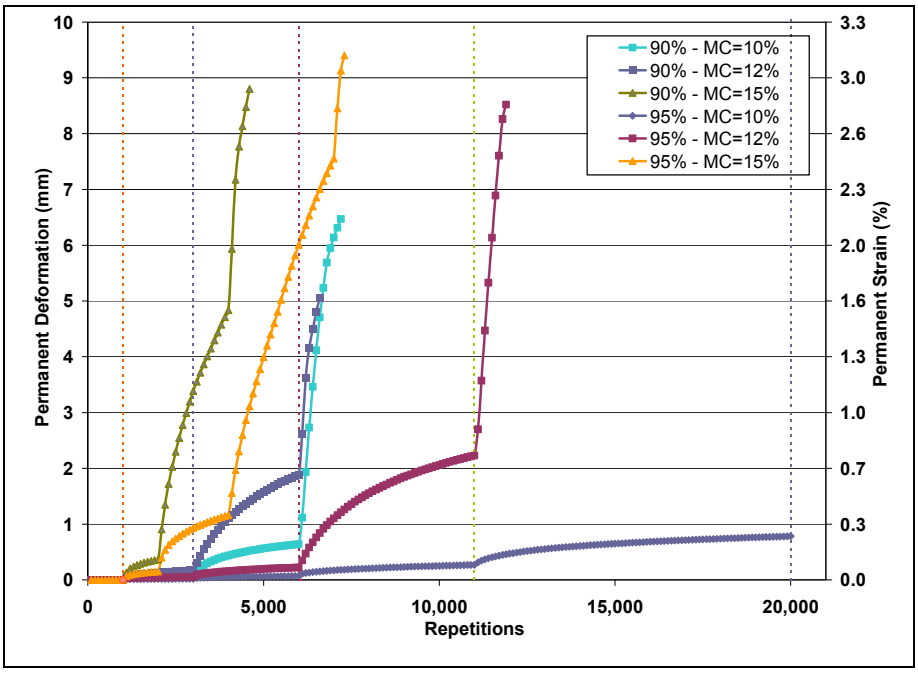

Figure 4.14: Silt: Permanent deformation using confining pressure of 14 kPa.

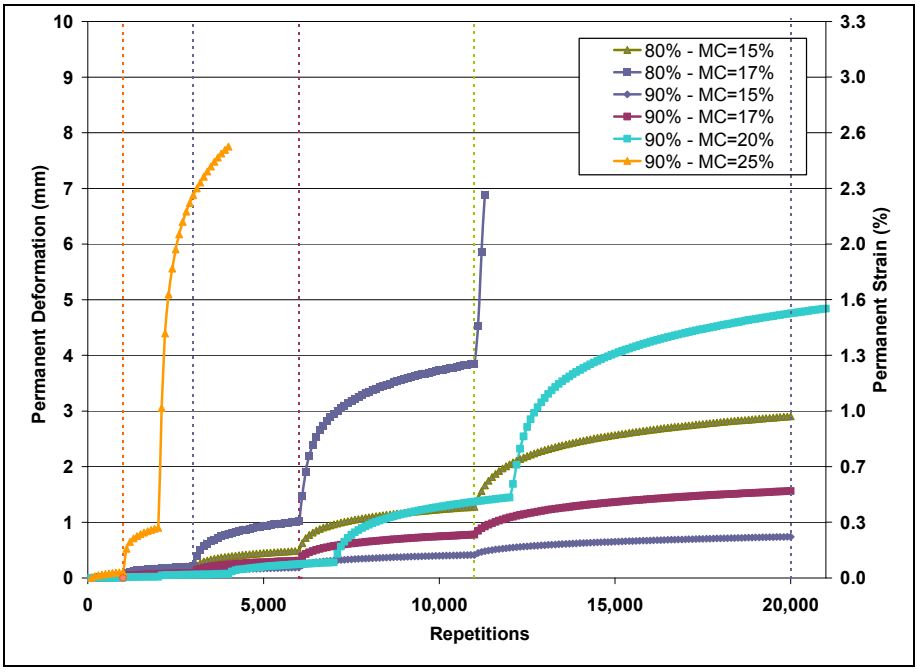

Figure 4.15: Clay: Permanent deformation using confining pressure of 14 kPa.

4.4 Summary

The results of tests on two different subgrade soils common in the Central Valley of California indicate that both soil types will add very little support to a pavement structure, and that the stiffness and the associated strength of the materials will decrease significantly as the moisture content increases. Any fully permeable pavement structure on these materials will need to compensate for this poor bearing capacity with thicker base and surfacing layers. Testing was not undertaken in the saturated condition given the already poor performance recorded at compaction moisture contents, and the difficulty in preparing specimens for testing (i.e. specimens "failed" before test could be started).

Chapter 5. Base Course Materials

5.1 Introduction

The base course separates the surface wearing course and subgrade materials and provides much of the bearing capacity in any pavement. On existing non-permeable pavements, they typically have a very dense grading and are usually compacted as densely as possible to provide a platform for the overlying wearing course layers and to provide the maximum possible structural integrity to the pavement. However, on fully permeable pavements, an open-graded base course is used to maximize water storage. This influences the degree of compaction and resultant strength that can be achieved. The base course will therefore typically need to be thicker to compensate for the lower strengths and stiffnesses associated with the less dense grading. Testing of base course materials focused on the stiffness of those materials.

5.2 Material Sampling

Four different commercially available aggregate samples of different geological origin (granite [two gradings], basalt, and alluvial) were sourced from three different suppliers in northern California. These materials were considered to be representative of sources in the Central Valley and coastal regions of the state. Photographs of the various aggregates are shown in Figure 5.1. The basalt and granite materials were sourced from a hard-rock quarry and were angular in shape. The basalt particles were predominantly flaky compared to the granite, which was predominantly blocky in shape. The alluvial material consisted of primarily smooth, rounded particles, although most had at least one crushed face.

Granite (1)

Granite (2)

Figure 5.1: Photographs of aggregates indicating size distribution and shape.

Basalt

Alluvial

Figure 5.1: Photographs of aggregates indicating size distribution and shape (cont.)

5.3 Test Results

5.3.1 Grading Analysis

The grading analysis was carried out following AASHTO Test Methods T 11 and T 27. The results for the four materials are shown in Figure 5.2. The results are compared with those discussed in the NAPA manual *(2)* and work done at the University of Illinois *(8,9,)* in Figure 5.3.

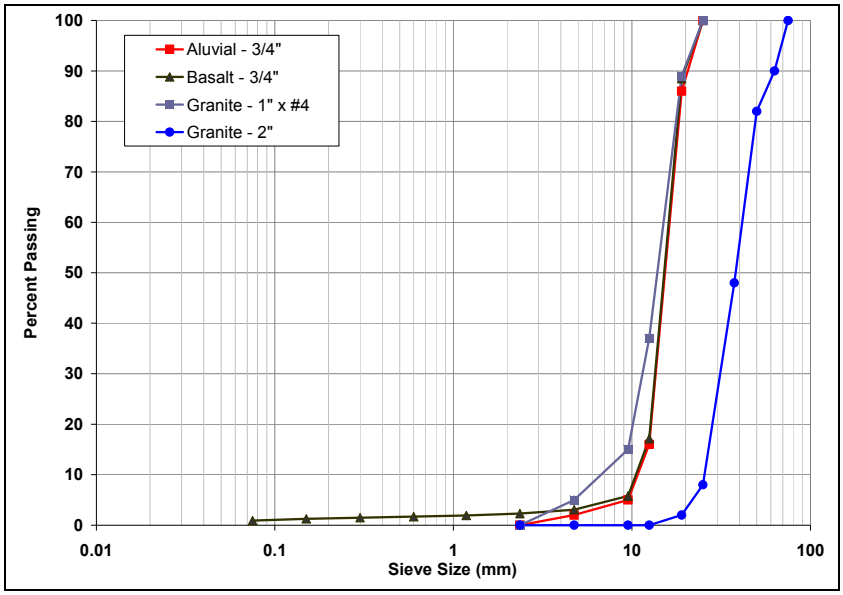

Figure 5.2: Grading analysis base course materials.

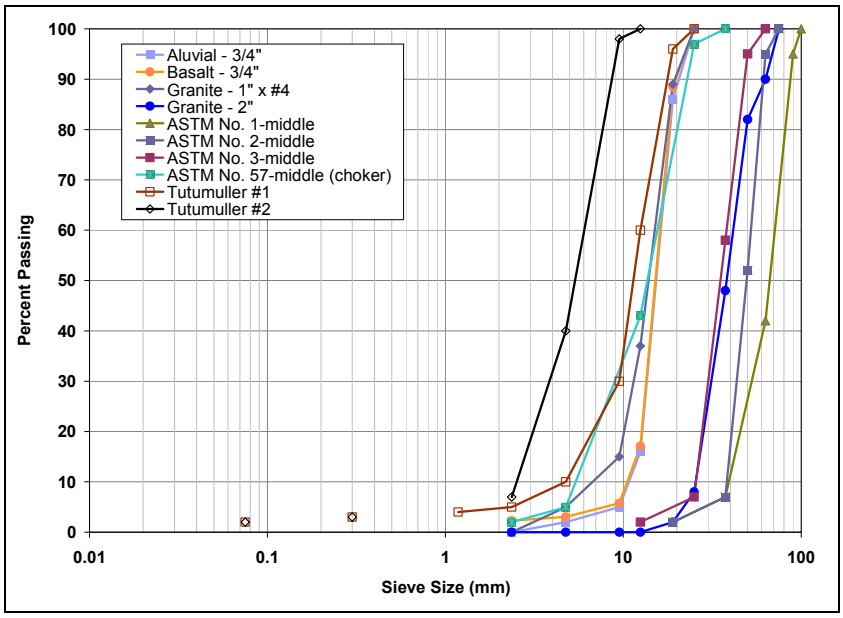

Figure 5.3: Grading analysis comparison with NAPA manual materials *(2)*.

The results show that the alluvial and basalt materials had a similar grading with no significant variation in particle sizes. The finer granite material (1 in. x #4) had a larger range of particle sizes. The coarse granite (similar to railway ballast) contained significantly larger aggregates than the other materials, with very little variation in particle size, and was closer to the aggregate size typically recommended in the literature *(2)*. Three of the four materials selected for testing were generally finer than those described in the NAPA manual *(2)*, with the exception of the ASTM No.57 material, which had a similar grading to the finer granite. The coarse granite had a similar grading to the ASTM No.3 material, both of which were finer compared to the ASTM No1 and No.2 materials.

5.3.2 Permeability

Permeability of the four aggregates was determined using ASTM-PS 129. All materials had a void ratio between 20 and 25 percent and all had permeabilities close to 0.1 cm/s. This permeability appears to be sufficient for typical California conditions, based on initial findings of a companion study investigate hydrological modeling of fully permeable pavements.

5.3.3 Resilient Modulus

Specimen Preparation for Triaxial Testing

There are no published specimen preparation or testing procedures for the triaxial testing of coarse open-graded materials. The AASHTO T-307 test method was therefore adapted as follows:

1. Weigh sufficient material for the preparation of one specimen (about 11 kg).
2. Place a thick rubber membrane inside the mold and place it on the vibration table.
3. Place the material into the mold in six separate lifts, rodding each lift 20 times to orient the material and optimize particle interlock. Weigh the remaining material.
4. Place the specimen on the testing frame.
5. Remove the mold from the specimen and measure height and diameter according to AASHTO T 307.
6. Position the transducers and test according to AASHTO T 307.

Specimen details for the four materials are summarized in Table 5.1. However, the coarse granite could not be tested as the aggregates were too large to prepare a satisfactory 152 mm specimen.

Table 5.1: Triaxial Specimen Details

Material	Mass (kg)	Diameter (mm)	Height (mm)	Density (kg/m^3)	Specific Gravity	Void Content (%)
Alluvial – ¾ in.	9.929	152	315	1,737	2.762	37
Basalt – ¾ in.	9.340	152	312	1,650	2.670	38
Granite – 1 in. x #4	10.275	152	318	1,781	2.761	36
Granite – 2 in.	8.890	152	304	1,612	2.761	42

Testing Sequence

Resilient modulus testing was carried out according to AASHTO T 307, but with the addition of one extra confinement sequence at the beginning of the test (00 in Table 5.2) to prevent premature disintegration of the specimen.

Table 5.2: Resilient Modulus Testing Sequence (Modified from AASHTO T-307)

Sequence No.	Confining Pressure, σ_3		Max. Dev. Stress, σ_d		No. of Load Applications
	(kPa)	(psi)	(kPa)	(psi)	
00	103.4	15	0	0	200 sec
0	103.4	15	103.4	15	500
1	20.7	3	20.7	3	100
2	20.7	3	41.4	6	100
3	20.7	3	62.0	9	100
4	34.5	5	34.5	5	100
5	34.5	5	68.9	10	100
6	34.5	5	103.4	15	100
7	68.9	10	68.9	10	100
8	68.9	10	137.9	20	100
9	68.9	10	206.8	30	100
10	103.4	15	68.9	10	100
11	103.4	15	103.4	15	100
12	103.4	15	206.8	30	100
13	137.9	20	103.4	15	100
14	137.9	20	137.9	20	100
15	137.9	20	275.8	40	100

Results

The average results of resilient modulus testing on the three materials are presented in Figure 5.4. The results show that there was very little difference in performance between the three material types, although the finer, more graded samples had a slightly higher resilient modulus, as expected. The resilient modulus values were considerably lower than those typically obtained from testing conventional dense-graded aggregate base course materials.

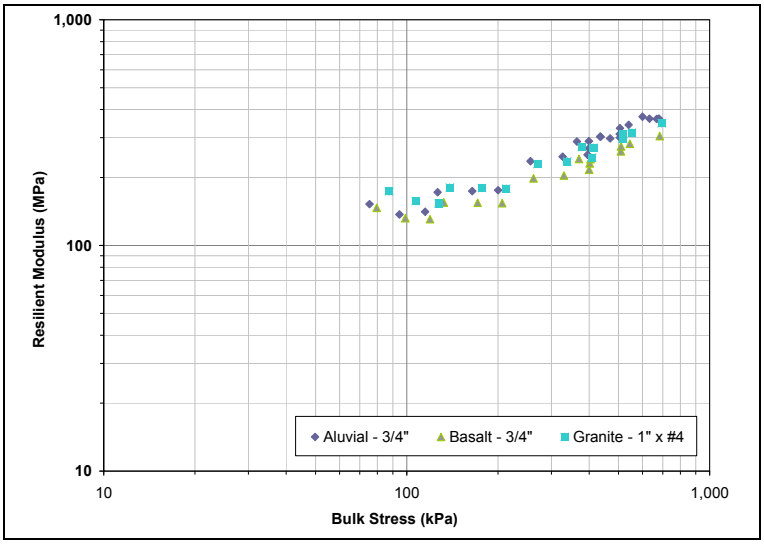

Figure 5.4: Resilient modulus of base materials.

The results were compared to a selection of other results from the literature *(8,9)* (Figure 5.5). The resilient moduli of the materials tested in this study generally fell between those tested in the other studies, but showed similar trends in terms of the effects of grading and particle size on resilient modulus.

The stress dependency parameters for the K-θ and Universal resilient modulus models, which will be used in the mechanistic-empirical pavement analyses, are listed in Table 5.3.

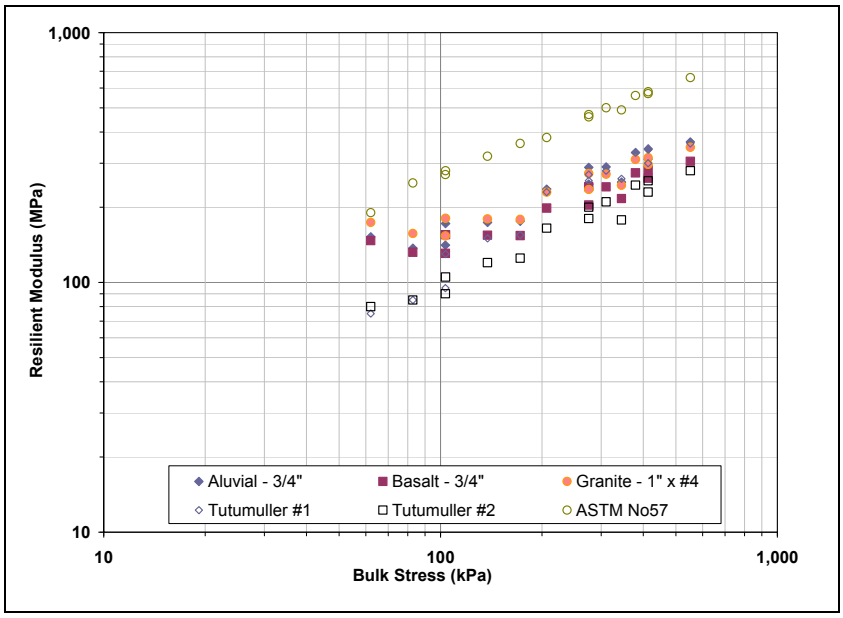

Figure 5.5: Resilient modulus comparison with results from literature *(8,9)*.

Table 5.3: Resilient Modulus Model Parameters

Material	K-θ Model			Universal Model			
	K_1	K_2	R^2	K_1	K_2	K_3	R^2
Aluvial – ¾ in	12.610	0.538	0.937	11.797	0.775	-0.267	0.993
Basalt – ¾ in	16.145	0.465	0.929	15.254	0.667	-0.228	0.983
Granite – 1 in x #4	21.274	0.440	0.926	20.175	0.628	-0.213	0.979
Tutumuller #1	3.075	0.776	0.959	2.556	1.040	-0.274	0.982
Tutumuller #2	5.658	0.620	0.964	4.788	0.858	-0.247	0.994
ASTM No57	21.624	0.544	0.992	21.536	0.550	-0.006	0.992

5.3.4 Dynamic Cone Penetrometer

Dynamic Cone Penetrometer (DCP) tests were carried out on the base course materials, confined in barrels to determine whether this equipment could be used as a rapid indicator of layer bearing capacity. Typical layer thicknesses anticipated in fully permeable pavements were assessed and the material was confined on the surface with a 25 mm thick steel plate to simulate an overlying layer.

All specimens were penetrated to a depth of 800 mm in 10 or less blows, indicating that the test set-up was not representative of a base layer on a typical roadway.

No attempt was made to relate the findings to bearing capacity or stiffness, since the models developed by a number of practitioners in the United States and internationally and derived from extensive comparisons

of DCP results with laboratory and field test results are all based on dense-graded, compacted materials and were therefore considered to be inappropriate for evaluating the materials assessed in this study.

5.4 Summary

The results of tests on four different commercially available permeable base-course aggregates indicate that these materials will probably provide sufficient support for typical traffic loads in parking lots, basic access streets and driveways, and on highway shoulders, whilst serving as a reservoir layer for the pavement structure. Although three of the four materials tested had smaller maximum aggregate sizes than those typically discussed in the literature, the permeability was still adequate for California rainfall events. The required thickness of the base and the expected structural performance in terms of the pavement structure will be discussed in a later report.

Chapter 6. Portland Cement Concrete Materials

6.1 Introduction

Portland cement concrete (PCC) materials are an alternative to hot-mix asphalt (HMA) as a wearing course. They provide a more rigid surface than HMA and are therefore typically more rut-resistant but more prone to cracking. As with HMA wearing courses, the material grading needs to be optimized to provide a balance between strength and permeability. The testing of PCC wearing course materials in this study focused on tensile, compressive, and flexural strengths and associated permeability. A phased approach was followed in that preliminary testing (Phase 1) was carried out on a broad range of gradings identified in the literature. This was followed by more comprehensive testing (Phase 2) on specimens prepared with the three most promising gradings identified in Phase 1. Additional testing (Phase 3) was then carried out to assess the effects of a number of other parameters including cement content and particle shape. A final phase of testing (Phase 4) to compare open-graded mixes with slabs with pre-cast/cast-in-place drainage holes was also undertaken.

6.2 Material Sampling

Three different commercially available aggregate samples of different geological origin (granite, basalt, and alluvial) were sourced from the same three suppliers discussed in Chapter 5. These materials were considered to be representative of sources in the Central Valley and coastal regions of the state. The first two phases of testing were carried out on the granite material, while Phase 3 testing was carried out on the basalt and alluvial materials.

6.3 Test Methods

Laboratory testing consisted of measurement of compressive strength, tensile strength, flexural strength, fatigue resistance, and permeability on prepared specimens. The bulk specific gravity and bulk density of the specimens were also measured to determine the air-void content of the specimens. AASHTO or ASTM standard test methods were followed during testing as shown in Table 6.1.

Table 6.1: Test Methods for PCC Materials

Test	Test Method	Preliminary Specimens	Comprehensive Specimens	Supplementary Specimens
Specimen preparation	ASTM C-31	30	33	18
Compressive Strength	ASTM C-39	30	15 (5 per mix)	9 (3 per mix)
Split Tensile Strength	AASHTO T-198	--	15 (5 per mix)	9 (3 per mix)
Flexural Strength	ASTM C-78	--	3 (1 per mix)	--
Fatigue Resistance	Mod ASTM C-78	--	3 (1 per mix)	--
Max. Specific Gravity	AASHTO T-209	29	--	6 (2 per mix)
Bulk Specific Gravity	AASHTO T-331	29	--	6 (2 per mix)
Air-void Content	AASHTO T-269	29	--	6 (2 per mix)
Permeability	ASTM PS 129-01	All specimens	All specimens	All specimens

6.4 Specimen Preparation

All concrete was mixed in a nine cubic foot electric concrete mixer using Type II portland cement. Water content was adjusted to obtain zero slump to better control the density of the concrete. The tamping rod method was chosen over the Modified Proctor method for compacting the specimens based on results and recommendations in the literature. Specimens were cured at 20°C in a wet cure room for 28 or 56 days, depending on the phase of testing. Bulk specific gravity and bulk density were determined after curing.

6.5 Phase 1: Preliminary Testing

The six gradations for preliminary testing were chosen to maximize the connected voids in the specimens and are summarized in Table 6.2 and Figure 6.1. The Bailey Method, often used in HMA mix design for optimizing air-void contents, was used for two of the gradations.

Table 6.2: Phase 1 Testing Mix Proportions.

Parameter		Mix Proportions (kg/m^3)					
		Mix 1 trial	Mix 2 9.5	Mix 3 4.75s	Mix 4 Bailey 1	Mix 5 Bailey 2	Mix 6 9.5+sand
Aggregate	12.5 mm	4.5	0.0	4.5	0.0	0.0	0.0
	9.5 mm	87.0	1,500.0	87.0	900.0	900.0	1,500.0
	4.75 mm	1,387.5	0.0	1,387.5	600.0	600.0	0.0
	2.36 mm	7.5	0.0	18.4	10.9	21.8	10.9
	1.18 mm	1.5	0.0	23.7	22.2	44.4	22.2
	0.6 mm	0.0	0.0	24.0	24.0	48.0	24.0
	0.3 mm	0.0	0.0	20.5	20.5	41.0	20.5
	0.15 mm	1.5	0.0	13.9	12.4	24.8	12.4
	0.075 mm	1.5	0.0	5.5	4.0	8.0	4.0
Cement	-	455.0	350.0	350.0	350.0	350.0	350.0
Water	-	98.0	105.0	98.0	98.0	98.0	98.0
W/C ratio	-	0.22	0.30	0.28	0.28	0.28	0.28

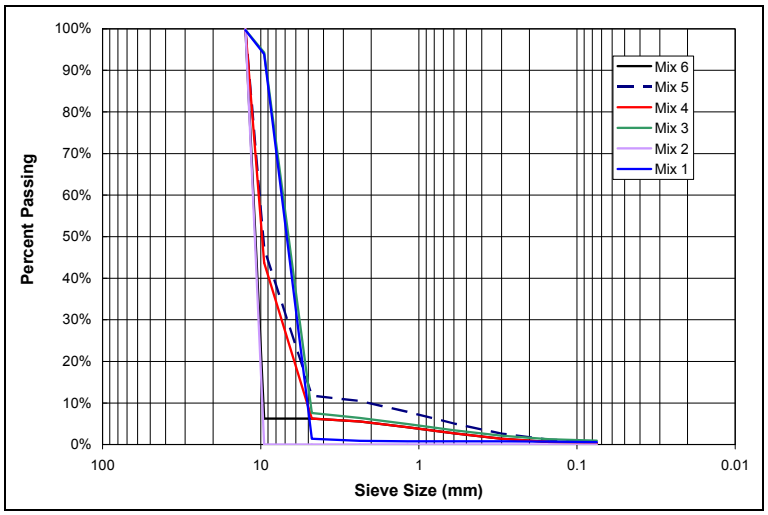

Figure 6.1: Gradations of six preliminary mix proportions.

Test results are summarized in Table 6.3 and Figure 6.2. The average permeability tended to increase with increasing air-void content and the compressive strength tended to decrease with increasing air-void content, as expected. The standard deviations for the permeability values were relatively large compared to the average values. This was attributed to variations in the interconnectivity of the voids between specimens. The air-void contents were similar within each of the mix gradations, but differed by up to 25 percent between gradations. Mix 2 (uniform gradation using 9.5 mm aggregate) had the highest air-void content, greatest permeability, and lowest compressive strength of all the specimens. Strengths were generally significantly lower than comparative typical dense-graded concrete. It should be noted that permeability is highly dependent on void connectivity and consequently high variability when testing laboratory specimens is expected.

Table 6.3: Test Results from Preliminary Testing

Mix	Air-Void Content (%)		Permeability (cm/s)		Compressive Strength (MPa)	
	Average	Std. Dev	Average	Std. Dev	Average	Std. Dev
1	29.8	0.00	4.52	2.94	4.48	0.33
2	35.4	0.94	6.75	3.75	1.45	0.35
3	31.7	0.63	5.23	0.97	2.71	0.38
4	30.7	2.00	5.84	3.06	4.33	1.58
5	28.6	0.53	3.97	1.46	5.06	0.72
6	29.1	1.27	4.53	2.48	3.99	0.72

Based on these results, Mixes 4, 5 and 6 were selected for more comprehensive testing. These mixes showed the best balance between strength and permeability. Initial results indicate that the permeability exceeded anticipated requirements and that the gradings could be densified (i.e. permeability reduced) to improve strength.

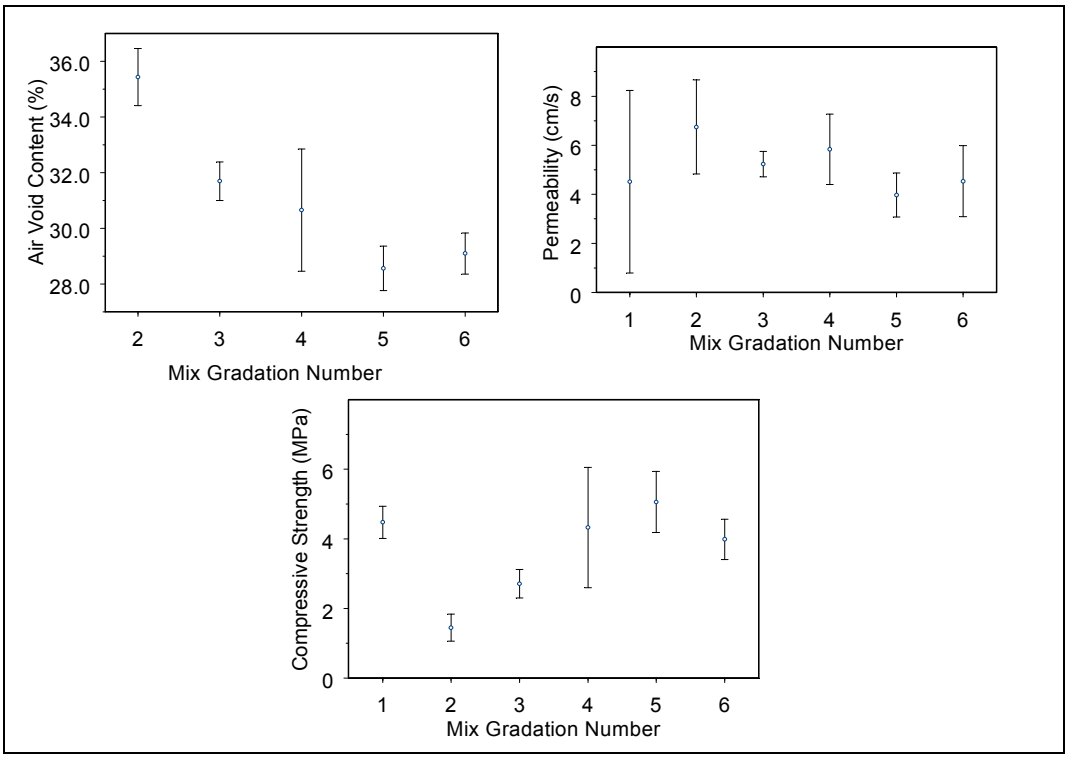

Figure 6.2: Test results from preliminary testing.

6.6 Phase 2: Comprehensive Testing

Based on the initial findings discussed in Section 6.5, the gradings for the selected mixes (Mixes 4, 5 and 6) were not altered. However, the cement contents were increased by 30 kg per mix in an attempt to increase the strengths. Water contents were also increased to raise the water/cement ratio. Attempts to produce mixes using lower water contents were unsuccessful due to poor workability. The revised mix proportions used in the second phase of testing are summarized in Table 6.4.

Table 6.4: Comprehensive Testing Mix Proportions.

Parameter		Mix Proportions (kg/m^3)		
		Mix 4 Bailey 1	Mix 5 Bailey 2	Mix 6 9.5+sand
Aggregate	9.5 mm	900.0	900.0	1,500.0
	4.75 mm	600.0	600.0	0.0
	2.36 mm	10.9	21.8	10.9
	1.18 mm	22.2	44.4	22.2
	0.6 mm	24.0	48.0	24.0
	0.3 mm	20.5	41.0	20.5
	0.15 mm	12.4	24.8	12.4
	0.075 mm	4.0	8.0	4.0
Cement	-	380.0	380.0	380.0
Water	-	120.0	121.0	128.0
W/C ratio	-	0.32	0.32	0.34

Test results are summarized in Table 6.5. Figure 6.3 provides a graphical display of the variance of strength with time, showing only a marginal increase in strength over the second 28 day curing period. The trend between tensile strength and permeability is shown in Figure 6.4, with a general decrease in tensile strength with increase in permeability evident, as expected.

The eight percent increase in cement content between the preliminary and comprehensive test specimens caused an increase of approximately 97 to 150 percent in compressive strength and a decrease in permeability of approximately 55 to 60 percent. An exception was the Bailey 1 mix, which had lower strengths compared to the other two mixes. The compressive strength of this mix only increased approximately 10 percent with the increase in cement content. The specimens did not gain a significant amount of additional strength between 28 and 56 days. Although the compressive strengths increased significantly with the higher cement content, they were still considerably lower than typical dense-graded mixes tested at the UCPRC in other projects (28-day compressive strengths of between 28 MPa and 30 MPa were obtained *[10]*).

Flexural strengths were also lower than comparative dense-graded mixes. The Bailey 2 and 9.5 + sand mixes had higher flexural strengths than the Bailey 1 mix. However, these strengths were about 1.2 MPa lower than strengths obtained on dense-graded mixes *(10)*.

Fatigue and coefficient of thermal expansion testing had not been completed at the time of preparing this report. Results and discussion will be provided in the final report.

Table 6.5: Average Strength and Permeability Values for Comprehensive Test Specimens

Mix	28 day Compressive Strength (MPa)		56 day Compressive Strength (MPa)		28 day Tensile Strength (MPa)		56 day Tensile Strength (MPa)		56 day Flexural Strength (MPa)		Permeability (cm/s)	
	Average	Std. Dev	Average	Std. Dev	Average	Std. Dev	Average	Std. Dev	Average	Std. Dev	Average	Std. Dev
Bailey 1	4.74	0.30	5.35	0.76	0.97	0.06	1.10	0.34	1.25	-	2.64	2.41
Bailey 2	9.95	1.48	9.58	0.01	2.03	0.14	2.25	0.10	2.33	-	1.62	1.02
9.5 + sand	9.97	0.84	11.28	0.11	2.56	0.37	2.39	0.03	2.35	-	1.81	1.05

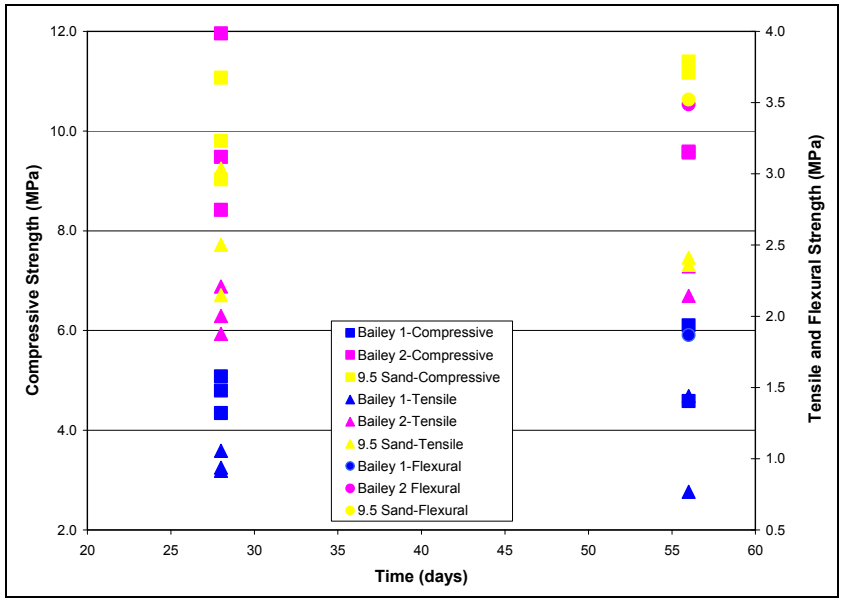

Figure 6.3: Strength vs. time for comprehensive specimens.

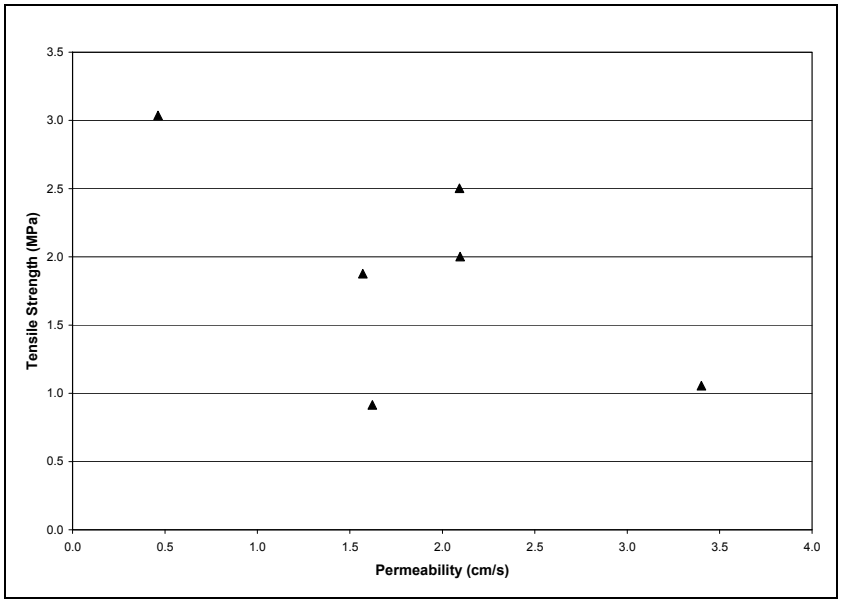

Figure 6.4: Tensile strength vs. permeability for comprehensive specimens.

6.7 Phase 3: Supplementary Testing

In this phase, the influence on performance of different aggregate type and additional cement was investigated. Two additional, different aggregate types and one additional cement content were investigated. The 9.5 mm aggregate-with-sand gradation (Mix 6) was chosen for this testing because it showed the best combination of strength and permeability in the Phase 2 testing. The revised mix proportions are summarized in Table 6.6. A slightly lower water/cement content ratio was used compared to the Phase 2 testing to assess the impact of this variable on workability, permeability, and strength.

Permeability was measured after 28 days of curing, while the compressive and tensile strengths were determined after 56 days of curing. The results are summarized in Table 6.7.

Table 6.6: Supplementary Testing Mix Proportions.

Parameter		Mix Proportions (kg/m^3)	
		Different Aggregate	Additional Cement
Aggregate	9.5 mm	1,500.0	1,500.0
	4.75 mm	0.0	0.0
	2.36 mm	10.9	10.9
	1.18 mm	22.2	22.2
	0.6 mm	24.0	24.0
	0.3 mm	20.5	20.5
	0.15 mm	12.4	12.4
	0.075 mm	4.0	4.0
Cement	-	380.0	410.0
Water	-	108.0	115.0
W/C ratio	-	0.28	0.28

Table 6.7: Test Results from Supplementary Testing

Mix	Compressive Strength (MPa)		Tensile Strength (MPa)		Permeability (cm/s)	
	Average	Std. Dev	Average	Std. Dev	Average	Std. Dev
Granite	5.59	-	4.44	-	1.78	1.14
Basalt	9.11	-	6.83	-	1.17	0.50
Alluvial	6.00	-	-	-	1.48	-
Add. cement	3.89	-	4.02	-	2.95	2.95

The Phase 3 compressive strengths were considerably lower than the Phase 2 (comprehensive testing) results for the granite material that was used in both tests as well as in the test to assess the influence of additional cement. The compressive strength of the alluvial material was higher than that of the granite in this phase of testing, but lower compared to the results obtained in the Phase 2 testing. Tensile strength values from the supplementary testing were between 1.5 and 2.5 times higher than the tensile strength values obtained in Phase 2.

Lower permeability values were obtained with the basalt and alluvial materials compared to the granite, probably due to the aggregate shape. Permeability increased with increasing cement content, which was not expected. The increase in permeability and decrease in strength for the specimens with additional cement was attributed to the lower water-to-cement ratio, which led to clumping of the cement during mixing and consequent poor coating of the aggregate. The drier clumps of cement also reduced the workability of the concrete, leading to poor consolidation during rodding.

It should be noted that although no durability testing was carried out, some stone loss was evident on most of the specimens during handling, indicating that the mixes are likely to have some susceptibility to raveling under traffic.

6.8 Phase 4: Precast/Cast-in-Place

Testing in this phase investigated the use of standard dense-graded portland cement concrete with precast or cast-in-place holes instead of an open-graded mix assessed in the earlier phases. Careful consideration needed to be given to the design of the holes to ensure sufficient strength, adequate drainage of the water, and safe use for bicycle, motorcycle, motor vehicle, and possibly pedestrian traffic. Testing focused on a comparison of tensile and flexural strengths between specimens with and without holes.

6.8.1 Beam Design

A number of hole/slot configurations were considered. However, the production of laboratory-scale slabs proved to be extremely difficult in terms of removing the mold from the slab, and damage to the slab during handling. These problems are not anticipated for slabs cast in place. Ultimately only one design was pursued. The general design followed is shown in Figure 6.5, based on 12 ft (3.6 m) wide by 15 ft (4.5 m) long slab. Drain holes are 2.0 in (50 mm) apart and 0.5 in (12.5 mm) in diameter and are staggered so as to catch all the water that flows across the slab in a transverse or longitudinal direction. The surface-to-void ratio, defined as the ratio between surface drainage area (holes) and total surface area, was 3.1 percent.

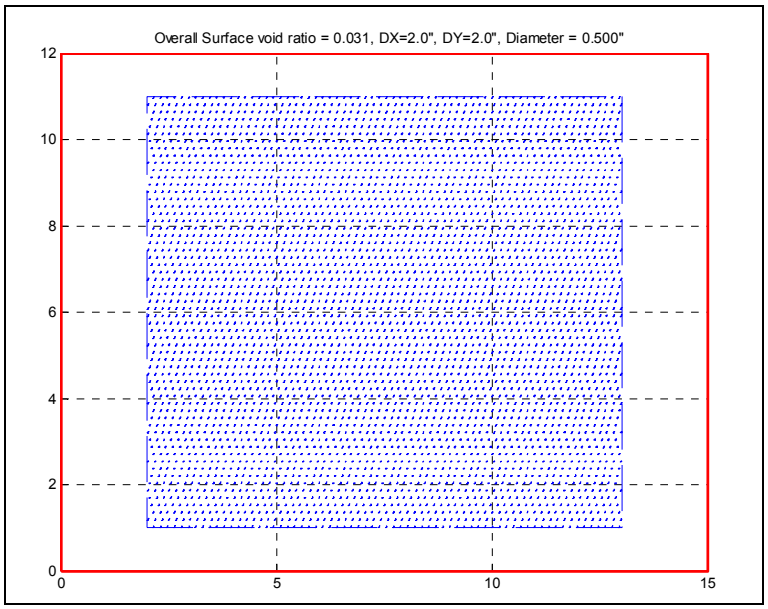

Figure 6.5: Top view of cast porous concrete pavement.

The design of the laboratory-scale beam, using actual hole size and hole spacing, is shown in Figure 6.6. The design was based on the assumption that at least five holes across the slab would be necessary to provide an indication of potential behavior in the field. Accommodating five holes across the beam plus sufficient space between the edge of the slab and the first set of holes required a beam width of 11 in (275 mm). A beam length of 37 in (925 mm) was used to maintain appropriate beam geometry. The depth of the beam was set at 6.0 in (150 mm), in line with standard laboratory practice for producing concrete beams.

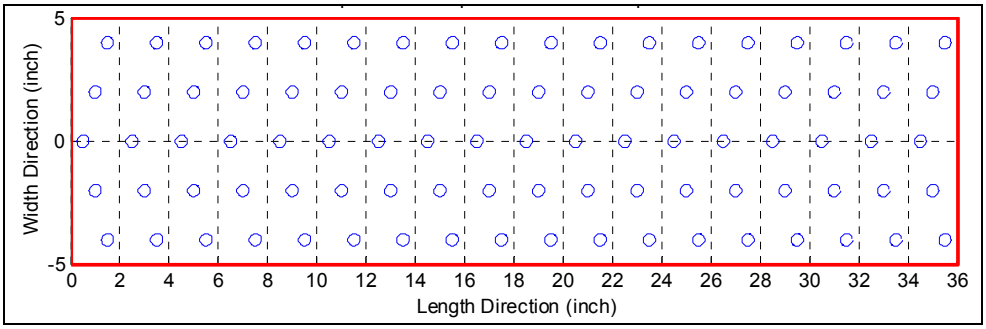

Figure 6.6: Top view of laboratory scale precast porous beam specimen.

6.8.2 Material Sampling

All testing was carried out with the alluvial materials discussed in the previous sections.

6.8.3 Beam Fabrication

Two custom wooden molds were fabricated to cast the specimens (Figure 6.7). This final design was selected after a number of earlier attempts that failed for a number of reasons including bending/alignment/breakages of the vertical dowels, problems with removing the mold after fabrication, poor distribution of the concrete in the mold (i.e. cavities around dowels and along beam edges), and damage to the specimen during handling after fabrication. The final design incorporates steel dowels with rubber pipe sleeves. Waterproof lubricants were applied between the rubber sleeves and steel dowels as well as the outside surface of the rubber sleeves. It is anticipated that full-scale construction would use plastic tubes for hole casting and that these tubes would remain in the concrete after casting.

A standard Caltrans half-inch maximum aggregate size design was used, although water contents were increased to improve flow within the mold and reduce the formation of cavities. Practice preparation revealed that a generally smooth specimen with no serious cavities could be produced (Figure 6.8).

Figure 6.7: Precast beam specimen molds.

Figure 6.8: Demolded precast beam specimen.

6.8.4 Testing

Testing of the beams had not been completed at the time of preparing this report. Results and discussion will be included in the final report.

6.9 Summary

Test results indicate a clear relationship between aggregate grading, cement content, water-to-cement ratio, and strength and permeability. All specimens tested exceeded the anticipated permeability requirements, indicating that aggregate gradings and cement contents can be adjusted to increase the

strength of the material whilst still retaining adequate water flow through the pavement. The water-to-cement ratio appears to be critical in ensuring good constructability and subsequent performance of the pavement. Although no durability testing was carried out, the mixes are likely to have some susceptibility to raveling under traffic.

Chapter 7. Hot-Mix Asphalt Materials

7.1 Introduction

Considerable research on porous asphalt has been undertaken in the past years by a number of institutions worldwide, and so-called open-graded friction courses are commonly used as a maintenance and pavement preservation strategy in California. Benefits include reduced splash and spray, improved skid resistance, and lower noise. However, all past research has been based on the existence of a dense-graded, impermeable layer underneath the porous asphalt layer, with water draining to the edge of the road and then into existing drainage structures.

The research discussed in this chapter describes the work undertaken to determine optimum mix designs for open-graded asphalt concrete wearing courses (or bases) for use in fully permeable pavements. This part of the study was undertaken in conjunction with another laboratory project being undertaken on behalf of Caltrans by the UCPRC to assess the properties of noise-reducing wearing courses, which allowed the testing of a far larger experimental matrix than originally planned. Testing was carried out in two phases. The first phase, carried out on 19 different mixes focused on permeability, rutting resistance, moisture sensitivity, and durability (resistance to raveling). The three best mixes were then subjected to fatigue testing to assess resistance to fatigue cracking, and to frequency sweep tests to characterize the influence of temperature and time of loading on stiffness.

7.2 Material Sampling

Three different commercially available aggregate samples of different geological origin (granite, basalt, and alluvial) were sourced from the same three suppliers discussed in Chapter 5 and Chapter 6. These materials were considered to be representative of sources in the Central Valley and coastal regions of the state. The European mix specimens sampled from the test track in Spain contained porphyry (course aggregates) and limestone (sand and fine fraction).

Five different binders, sourced from two different refineries, representing those typically used in California and other states were used in this study:

- PG64-16. This is a standard PG grade used in California and is widely used for open-graded mixes, since it is the specified grade when placement temperatures are greater than 21°C (70°F) in the North Coast, Low Mountain and South Mountain regions (Table 632.1 of the *Highway Design Manual*, per *Design Information Bulletin 86*, November 30, 2006). It is also widely used where

PG64-10 binders are specified (e.g. South Coast, Central Coast, and Inland Valley regions), since it exceeds the specifications of the PG64-10, but allows the refineries to save costs by producing one instead of two binders. PG64-16 is also the base stock binder for most of the rubberized asphalt specified by Caltrans.

- PG58-34PM. This is a standard PG grade used in California, and is the recommended grade for open-graded wearing courses in all regions of the state when the placement temperature is less than 21°C (70°F). The PM indicates that the binder is polymer modified. It is softer than PG64-16 at both high and low temperatures.
- PG76-22PM. This is a much stiffer binder than PG58-34PM at both high and low temperatures, and is also polymer modified. This binder is specified in Georgia DOT Standard Specifications for use in open-graded friction course mixes, which have reportedly performed very well and deserved assessment for use in California.
- PG76-22TR. This binder has similar stiffness to PG76-22, but is modified with between 10 and 15 percent recycled tire rubber instead of polymer. The rubber is blended into the binder at the refinery and is known as terminal blend rubberized asphalt binder.
- Asphalt Rubber. Asphalt rubber binders typically contain between 15 and 20 percent recycled tire rubber (19 percent in this study). These binders are produced at the asphalt plant using a wet process.

7.3 Mix Designs

The mix designs used in the study were selected from a comprehensive literature search on the topic, past experience in California, as well as some experimentation. The mixes tested in the first phase are summarized in Table 7.1. The D125 mix is a Caltrans conventional dense-graded mix included for comparison with the permeable open-graded mixes. The G125, RW95 and AR95 mixes were tested in Phase 2, together with a European mix not tested in Phase 1 (these specimens were sawn from a test track in Spain and shipped to UCPRC for another project, but had sufficient permeability to warrant testing in this study).

Mix designs for all of the open-graded mixes, except the Georgia and Arizona mixes, were performed following California Test Method CT-368, (*Standard Method for Determining Optimum Bitumen Content (OBC) for Open-Graded Asphalt Concrete*). In this test, the binder contents are determined based on the calculation of the approximate bitumen ratio determined from surface area estimates calculated from the aggregate gradation, and a "drain-down" test. The binder contents for the mixes with rubberized asphalt binders were also determined following CT-368, in which the binder content determined for conventional binders is increased by a factor of 1.2 for rubberized binders. The mix design for the dense-graded control mix was performed following Caltrans standard practice. Mix design for the Georgia mix was performed following Georgia test method GDT-114. Mix design for the Arizona mix followed a method documented in the literature.

Table 7.1: Mix Designs used in Phase 1 and Phase 2 Testing

Mix ID	Mix Description			
	Aggregate	Max size (mm)	Binder	Comments
D125	Basalt	12.5	PG64-16	Dense-graded control mix. All other mixes are open-graded.
RW19		19.0	PG64-16	-
RW125		12.5	PG64-16	-
RW95		9.5	PG64-16	-
RW475		4.75	PG64-16	-
AR95		9.5	AR	-
AR475		4.75	AR	-
AR475P		4.75	AR	Coarser aggregate than other 4.75 mm gradations.
P475LM		4.75	PG64-16	Contains hydrated lime for moisture resistance.
TR475		4.75	PG76-22TR	-
P58LF		4.75	PG58-34PM	Contains cellulose fibers to hold binder in mix and hydrated lime for moisture resistance.
P475		4.75	PG76-22PM	-
G125		12.5	PG76-22PM	Georgia DOT mix. Coarser gradation than Caltrans 12.5 mm. Contains mineral fibers to hold more binder in mix and hydrated lime for moisture resistance.
AZ95		9.5	AR	Arizona mix. Slightly finer gradation than Caltrans 9.5 mm. Contains hydrated lime for moisture resistance.
E8		8.0	PG64-16	Danish mix. Contains some cellulose fibers to hold more binder in mix.
PG95T	Aluvial	9.5	PG64-16	-
AR475T		4.75	AR	-
AR95W	Granite	9.5	AR	-
PG475W		4.75	PG64-16	-
Cedex	Porphyry	12.5	N/A	Spanish mix. Binder was classified as BM-3c.

Aggregate gradations for each mix are shown in Table 7.2. The 12.5 mm, 9.5 mm and 4.75 mm open gradations are the same for each maximum size aggregate to permit comparison of other variables, except for the Arizona, Georgia, Danish and AR475P mixes.

Table 7.2: Aggregate Gradations of Mixes Tested

Mix ID	Percent Passing										NMAS[1] (mm)
	19-mm	12.5-mm	9.5-mm	4.75-mm	2.36-mm	1.18-mm	0.6-mm	0.3-mm	0.15-mm	0.075-mm	
D125	100	97.5	87.5	62.5	46	35	22.5	16	9	5	12.5
RW19	95	54	36	20	15	10	7	5	4	2	19.0
RW125	100	97.5	83.5	32.5	12.5	5	5	4	3	1.5	12.5
RW95	100	100	95	32.5	12.5	5	5	4	3	1.5	9.5
RW475	100	100	100	91	14	12	10	8	7	6	4.75
AR95	100	100	95	32.5	12.5	5	5	4	3	1.5	9.5
AR475	100	100	100	91	14	12	10	8	7	6	4.75
AR475P	100	100	100	65	14	12	10	7	6	5	4.75+
P475LM	100	100	100	91	14	12	10	8	7	6	4.75
TR475	100	100	100	91	14	12	10	8	7	6	4.75
P58LF	100	100	100	91	14	12	10	8	7	6	4.75
P475	100	100	100	91	14	12	10	8	7	6	4.75
G125	100	92.5	65	20	7.5	5	5	4	3	3	12.5
AZ95	100	100	100	40	9	5	4	3	2	2	9.5
E8	100	100	100	29	9	8	8	8	8	8	8.0
PG95T	100	100	95	32.5	12.5	5	5	4	3	1.5	9.5
AR475T	100	100	100	91	14	12	10	8	7	6	4.75
AR95W	100	100	95	32.5	12.5	5	5	4	3	1.5	9.5
PG475W	100	100	100	91	14	12	10	8	7	6	4.75
Cedex[2]	100	100	80	24	19	-	10	-	-	7	N/A

[1] Nominal maximum aggregate size [2] Gradings are approximate, converted from European metric sieve sizes.

The binder contents, lime contents, filler contents, and mixing and compaction temperatures are shown in Table 7.3, together with the Fineness Modulus, Coefficient of Curvature (C_c) and Coefficient of Uniformity (C_u) for each mix.

The Fineness Modulus is a measure of the uniformity of the aggregate gradation. The higher the fineness modulus, the coarser the asphalt mix (a higher percentage of coarse material) and the more uniform the gradation.

The Coefficient of Curvature (C_c) is a measure of the shape of a gradation curve. In the Unified Soil Classification System (USCS), a Coefficient of Curvature value between one and three is considered to be well graded. The Coefficient of Curvature is defined as:

$$C_c = D30^2/(D10 * D60) \quad (7.1)$$

Where D10 is the sieve size (mm) through which 10 percent of the aggregate passes
D30 is the sieve size (mm) through which 30 percent of the aggregate passes
D60 is the sieve size (mm) through which 60 percent of the material passes.

The Coefficient of Uniformity (C_u = D60/D10) is used to distinguish between open- and more dense graded mixes. Lower coefficients indicate that most of the material is approximately the same size, resulting in a uniform or open gradation, while higher values indicate that the gradation has a range of particle sizes resulting in a more well-graded or dense-graded mix.

Table 7.3: Properties of Mixes Tested

Mix ID	Binder Content (%)	Fiber[1] (%)	Hydrated Lime (%)	Mixing Temp (ºC)	Compact Temp (ºC)	Fineness Modulus	C_c[2]	C_u[3]
D125	6.0	0	0	144	125	4.22	1.19	25.60
RW19	5.0	0	0	135	125	6.08	0.70	2.14
RW125	5.9	0	0	135	125	5.55	1.38	3.72
RW95	5.9	0	0	135	125	5.43	1.47	3.48
RW475	7.9	0	0	135	125	4.58	0.91	1.60
AR95	7.1	0	0	163	149	5.43	1.47	3.48
AR475	9.5	0	0	163	149	4.58	0.91	1.60
AR475P	8.4	0	0	163	149	4.86	0.91	1.91
P475LM	7.9	0	1.5	135	125	4.58	0.91	1.60
TR475	9.5	0	0	163	149	4.58	0.91	1.60
P58LF	7.9	0.30 CF	1.5	155	138	4.58	0.91	1.60
P475	7.9	0	0	163	149	4.58	0.91	1.60
G125	6.3	0.40 MF	1.4	165	160	5.91	1.32	3.16
AZ95	9.2	0	1.0	163	149	5.37	1.03	2.60
E8	6.4	0.25 CF	1.5	135	125	5.30	1.37	2.75
PG95T	5.9	None	0	135	125	5.43	1.47	3.48
AR475T	9.5	None	0	163	149	4.58	0.91	1.60
AR95W	7.1	None	0	163	149	5.43	1.47	3.48
PG475W	7.9	None	0	135	125	4.58	0.91	1.60
Cedex	5.3	None	None	N/A	N/A	N/A	N/A	N/A

[1] CF = Cellulose Fiber and MF = Mineral Fiber [2] C_c = Coefficient of Curvature [3] C_u = Coefficient of Uniformity

In the basalt aggregate mixes, the binder contents increase with decreasing aggregate maximum size (e.g., RW19, RW125, RW95 and RW475). This is attributed to smaller size aggregates having a larger surface area-to-density ratio, and allows for more binder in the mix for a given mass of aggregate. The increase in binder content for asphalt rubber binders using the Caltrans open-graded mix design procedure can be seen by comparing RW475 (conventional binder) with AR475 (rubberized) and RW95 (conventional binder) with AR95 and AR95W (both rubberized).

7.4 Test Methods

Laboratory testing included measurement of permeability, shear, moisture sensitivity, and durability on prepared specimens. Limited beam fatigue and flexural frequency sweep testing was then carried out on the three mixes with the best performance in the other tests. Only three mixes were selected due to the time and complexity of fatigue testing, and the limited time available for this testing. The bulk specific

gravity and bulk density of the specimens were also measured to determine the air-void content of the specimens. AASHTO or ASTM standard test methods were followed during testing as shown in Table 7.4. Permeability testing is illustrated in Figure 7.1

Table 7.4: Test Methods for Asphalt Materials

Attribute	Test	Test Method
Permeability	Permeability	ASTM PS 129-01
Rutting resistance	Repeated Simple Shear Test	AASHTO T-320
Fatigue cracking resistance	Beam fatigue	AASHTO T-321
Moisture sensitivity	Hamburg Wheel Track	AASHTO T-324
Raveling resistance	Cantabro Test	ASTM D7064 x2
Max. Specific Gravity	Max. Specific Gravity	AASHTO T-209
Bulk Specific Gravity	Bulk Specific Gravity	AASHTO T-331
Air-void Content	Air-void Content	AASHTO T-269

Figure 7.1: Permeability testing on compacted slabs.

7.5 Test Results

The results for each set of tests are discussed in the following sections. Results shown are average values of the replicates. Plots include a bar indicating plus and minus one standard deviation variability of the results. Ranked results for permeability, moisture sensitivity, and rutting resistance (shear strength) are summarized in Table 7.5 and Table 7.6. Testing of raveling resistance and fatigue cracking resistance had not been completed at the time of preparing this report. Results will be presented in the final report.

Table 7.5: Ranked Results of Permeability, Moisture Sensitivity, and Rutting Resistance Tests.

Permeability (cm/s)			Moisture Sensitivity (Hamburg Wheel Track) (Repetitions to 10 mm rut)			Rutting Resistance (Shear Modulus) (MPa)		
Mix	**Average**	**Std Deviation**	**Mix**	**Average**	**Std Deviation**	**Mix**	**Average**	**Std Deviation**
D125	0.0009	0.0007	PG475W	317	159.1	P58LF	29.2	6.6
TR475	0.0284	0.0054	PG95T	377	88.4	P475	56.7	0.0
AZ95	0.0337	0.0067	RW125	425	77.8	TR475	57.5	6.0
P475	0.0529	0.0094	P475LM	681	51.6	PG95T	63.5	6.1
AR95W	0.0581	0.0170	RW95	725	318.2	AR475P	63.7	6.9
PG475W	0.0582	0.0102	E8	861	139.3	AR475T	63.9	1.6
P58LF	0.0638	0.0377	RW475	919	128.7	AR95W	65.0	2.3
AR475	0.0640	0.0559	TR475	2,013	108.9	AR475	65.3	0.0
AR475P	0.0758	0.0194	AR475	2,565	233.3	RW125	65.8	1.2
P475LM	0.0865	0.0287	P58LF	2,827	243.9	AZ95	66.9	0.6
AR475T	0.0919	0.0294	AR475P	2,930	21.2	RW95	69.4	3.3
AR95	0.1103	0.0244	AR95	3,030	169.7	RW475	92.9	2.1
RW475	0.1714	0.0211	AR475T	3,200	0.0	G125	93.9	1.0
PG95T	0.2144	0.0677	AZ95	3,967	272.2	E8	104.8	2.8
E8	0.2551	0.0486	P475	4,482	944.0	RW19	110.2	37.3
RW125	0.3006	0.0866	D125	5,170	650.5	PG475W	120.3	4.7
G125	0.3120	0.0807	RW19	5,250	424.3	P475LM	123.0	9.8
RW95	0.3223	0.1174	AR95W	6,222	328.8	D125	369.8	0.0
RW19	0.5833	0.3252	G125	17,981	3,119.8	AR95	-	-

Table 7.6: Ranked Results of Raveling Resistance, Flexural Stiffness, and Fatigue Resistance Tests.

Raveling Resistance (% Loss)			Flexural Stiffness (MPa)			Fatigue Resistance (Fatigue Life)		
Mix	**Average[1]**	**Std Deviation**	**Mix**	**Average**	**Std Deviation**	**Mix**	**Average**	**Std Deviation**
P58LF	2.4	**Not determined for summation of three conditions**	**Testing not complete at time of preparing report**					
AR475T	2.7							
TR475	3.6							
AR475P	8.1							
P475	10.4							
PG475W	12.3							
P475LM	17.1							
AR475	19.4							
RW475	20.2							
AZ95	20.3							
D125	20.9							
AR95W	28.3							
G125	32.9							
RW125	45.8							
PG95T	50.9							
AR95	53.2							
E8	54.7							
RW95	59.1							
RW19	63.2							

[1] Summation of three conditions (unaged, aged, and freeze-thaw cycle)

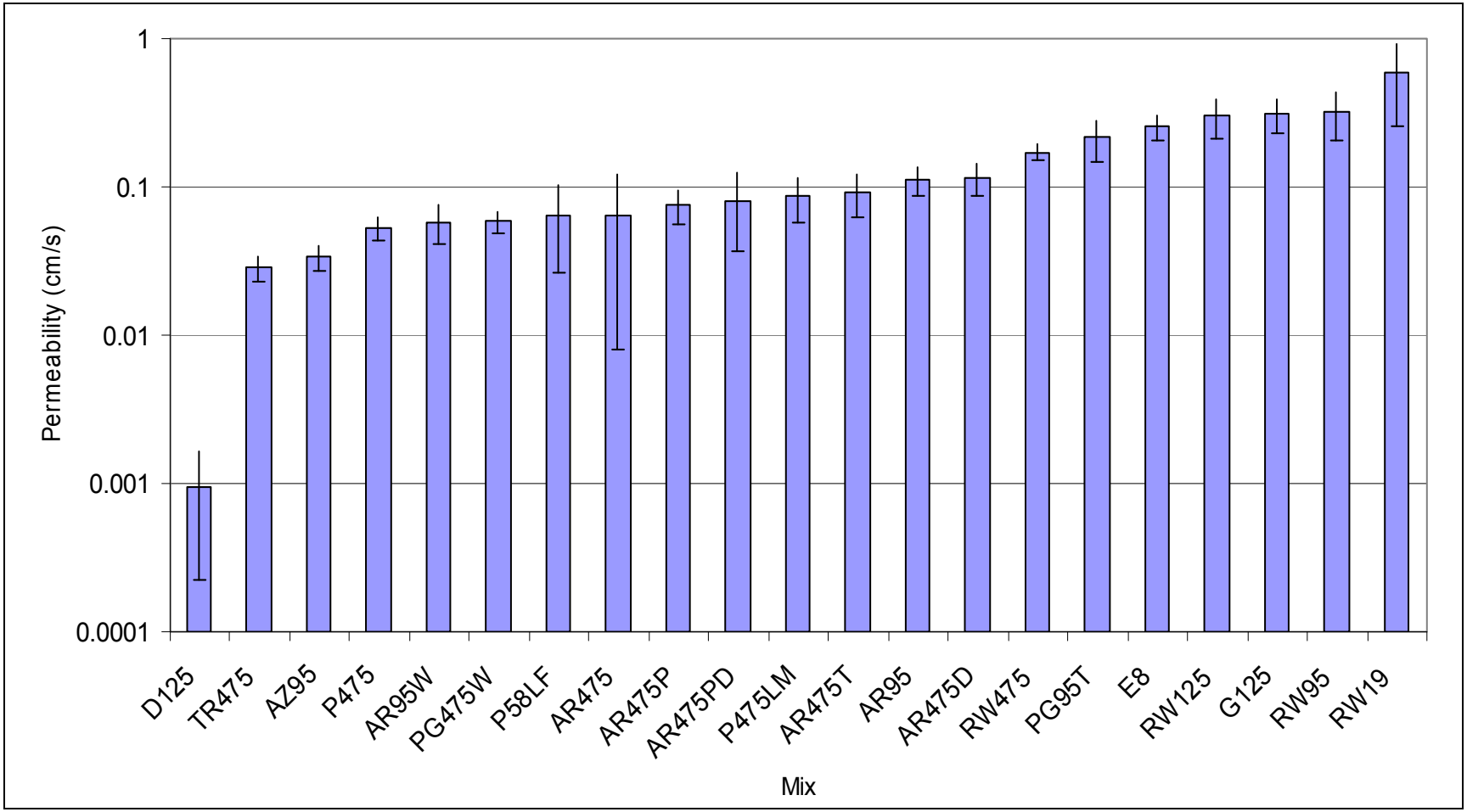

Figure 7.2: Summary plot of ranked permeability results for all mixes.
(Note log scale for permeability)

7.5.1 Permeability

Permeability results for all mixes are plotted in Figure 7.2. Comparisons with preliminary results from a parallel study of hydraulic calculations for pervious pavements indicates that a minimum permeability of 0.1 cm/second would be needed for typical rainfall events in California, and with multiple traffic lanes draining into a 3.0 m (10 ft) wide shoulder. Many of the mixes included in this study have permeabilities near that value.

Variables that will need to be used with these test results to determine which mixes will provide sufficient permeability include the extent of clogging over time (being investigated in the parallel study), and the number of lanes of traffic that need to be drained. The permeability for the control dense-graded mix (D125) is shown for comparison.

Figure 7.3 shows the comparison of the aggregate size for open-graded mixes with four aggregate sizes (19, 12.5, 9.5 and 4.75 mm [3/4, 1/2, 3/8 inch, and #4 sieves]). The results show that permeability tends to increase with increasing aggregate size. However, all of the mixes with conventional PG64-16 binder appeared to have sufficient initial permeability.

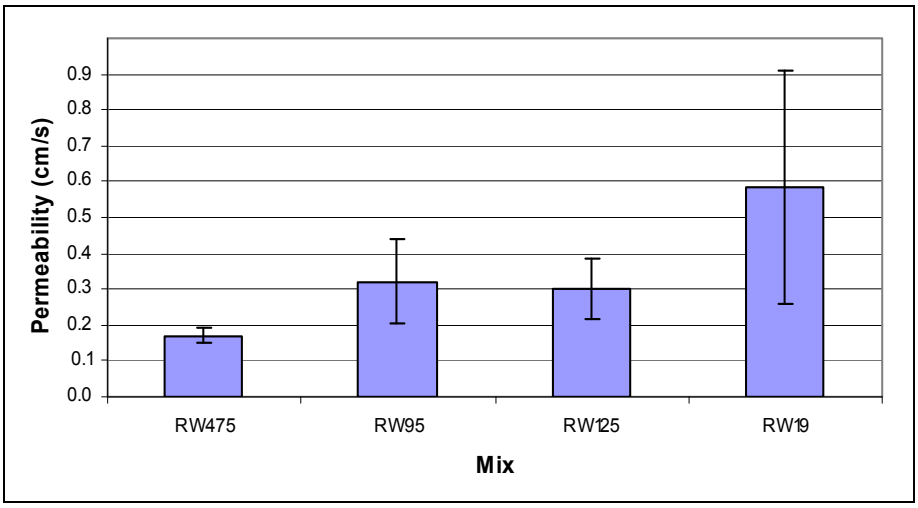

Figure 7.3: Comparison of effect of maximum aggregate size on permeability.
(Results for mixes with basalt aggregate and PG64-16 binder)

Figure 7.4 shows the comparison of mixes with different binders and 4.75 mm and 9.5 mm open-graded aggregate gradations. Permeability of the higher binder content asphalt rubber 9.5 mm mix (AR95) was lower than that of the same mix with conventional binder (RW95). Mixes with polymer modified binders

and with fibers also tended to reduce the permeability of the 4.75 mm mixes compared with the conventional binder mix (RW475).

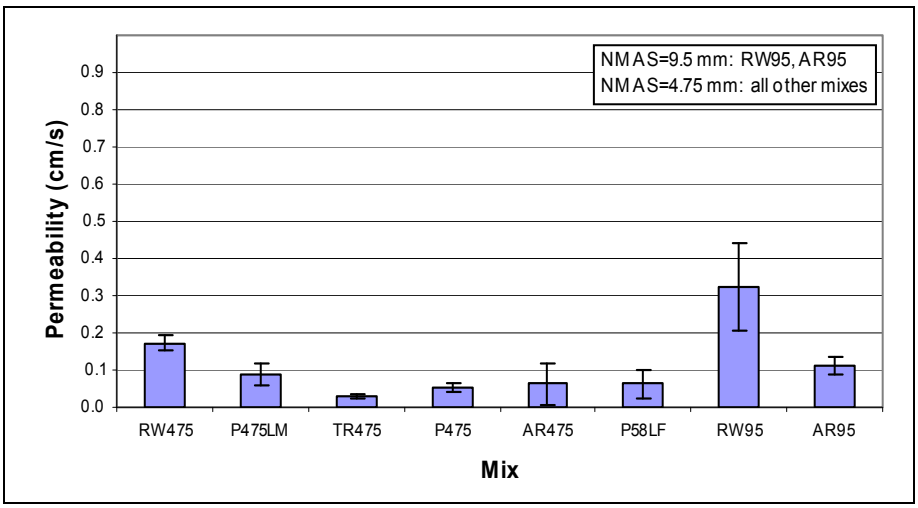

Figure 7.4: Comparison of effect of different binders on permeability.
(Results for mixes with basalt aggregate and 4.75 mm and 9.5 mm maximum aggregate size)

Figure 7.5 shows that additional compaction to obtain an air-void content of approximately 15 percent (instead of between 18 and 22 percent) did not decrease the permeability of the two 4.75 mm mixes with asphalt rubber binder.

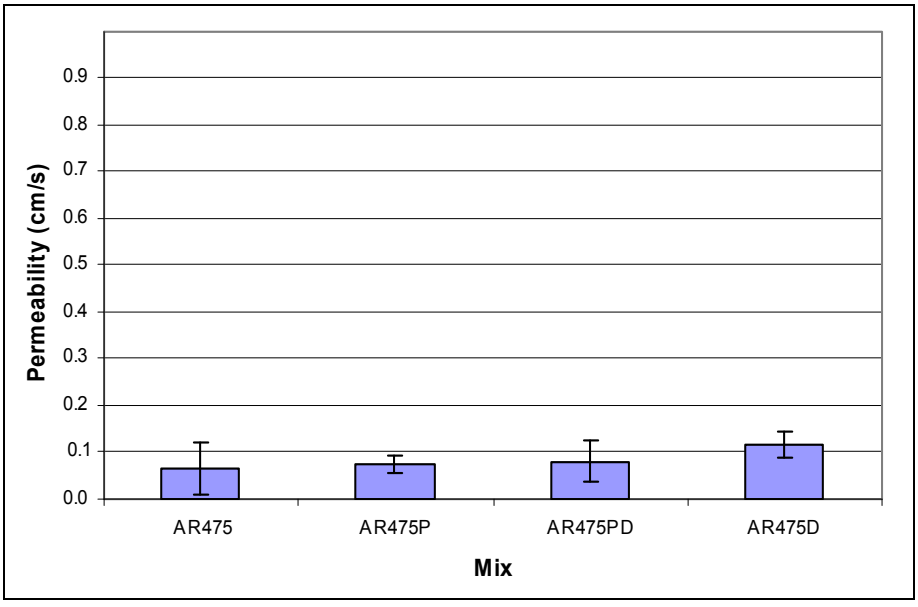

Figure 7.5: Comparison of effect of better compaction on permeability (4.75 mm mixes).

Figure 7.6 plots permeability against aggregate type. There was no consistent or significant trend of permeability in terms of aggregate source, although both of the mixes with granite aggregates had somewhat lower permeabilities than the corresponding mixes with basalt aggregate. This was attributed to the different shapes of the two aggregate sources.

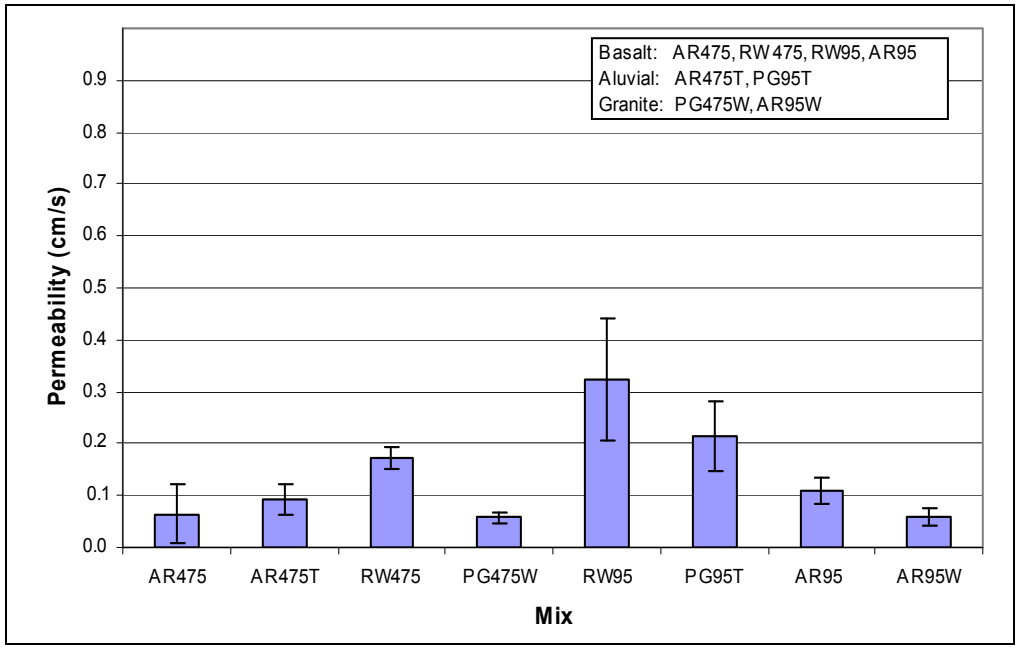

Figure 7.6: Comparison of effect of different aggregate types on permeability.
(Results for PG64-16 and asphalt rubber mixes with 4.75 mm and 9.5 mm maximum aggregate sizes)

7.5.2 Moisture Sensitivity

Hamburg Wheel Tracking Test (HWTT) results for all mixes are shown in Figure 7.7. It is interesting to note that the Georgia DOT open-graded mix (G125) had the best results, even higher than those of the control dense-graded mix, despite having nearly the highest permeability. This was attributed to the polymer-modified binder and use of fibers. Other open-graded mixes that had better HWTT results than the control mix were AR95W (attributed to rubberized binder) and RW19 (attributed to larger aggregate size).

Figure 7.8 shows the effects of aggregate size with the control mix (D125) for comparison. Generally the open-graded mixes had less rutting and moisture sensitivity resistance at high temperatures under soaked conditions compared to the dense-graded mix under the same conditions, which is expected.

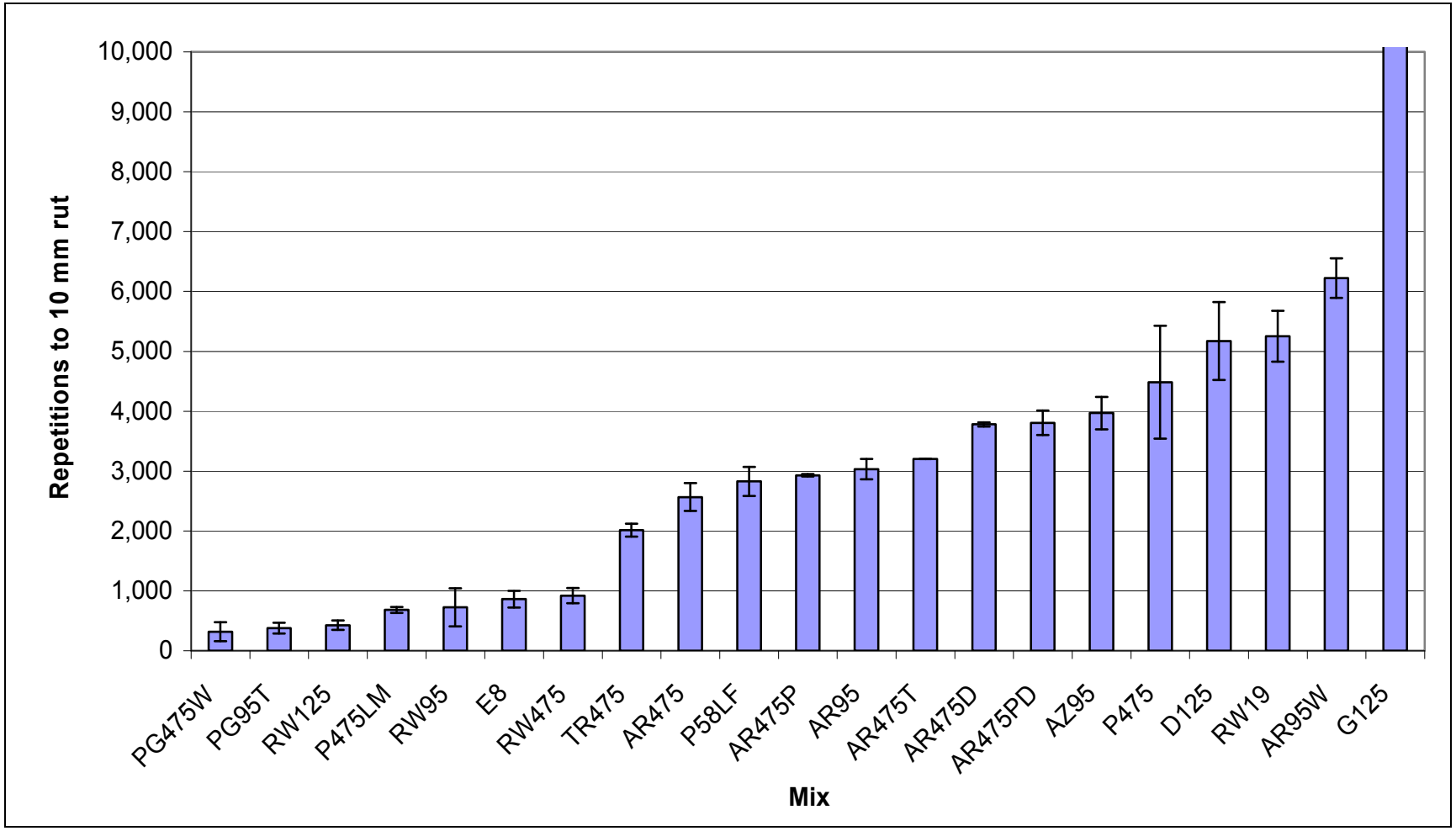

Figure 7.7: Summary plot of ranked HWTT results for all mixes.

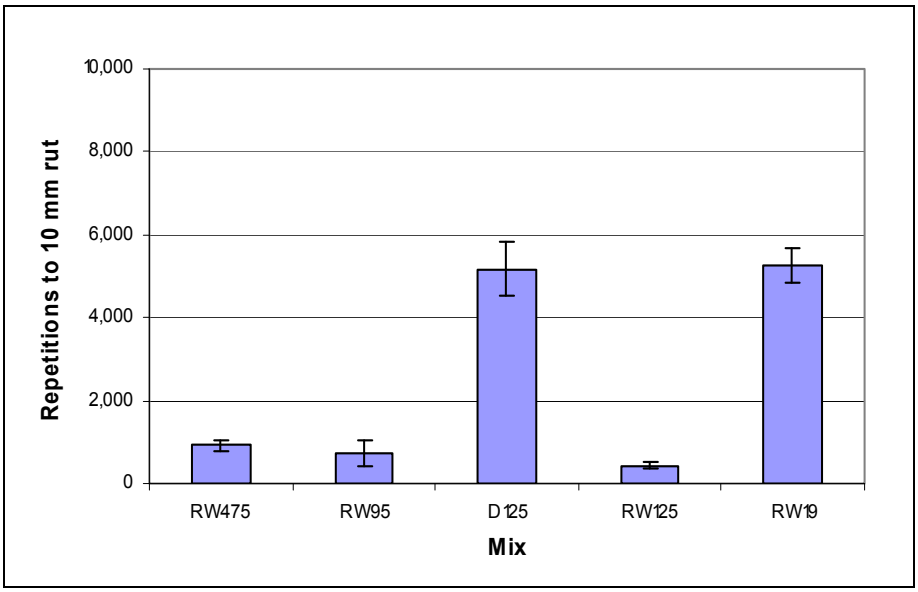

Figure 7.8: Comparison of effect of maximum aggregate size on moisture sensitivity.
(Results for mixes with basalt aggregate and PG64-16 binder)

Figure 7.9 shows the results for mixes with different binders and 4.75 mm and 9.5 mm gradations. The polymer-modified mix and asphalt rubber mixes appeared to offer superior resistance for the 4.75 mm mixes. Similarly the asphalt rubber mix appeared to be better than the same mix with conventional binder for the 9.5 mm mixes.

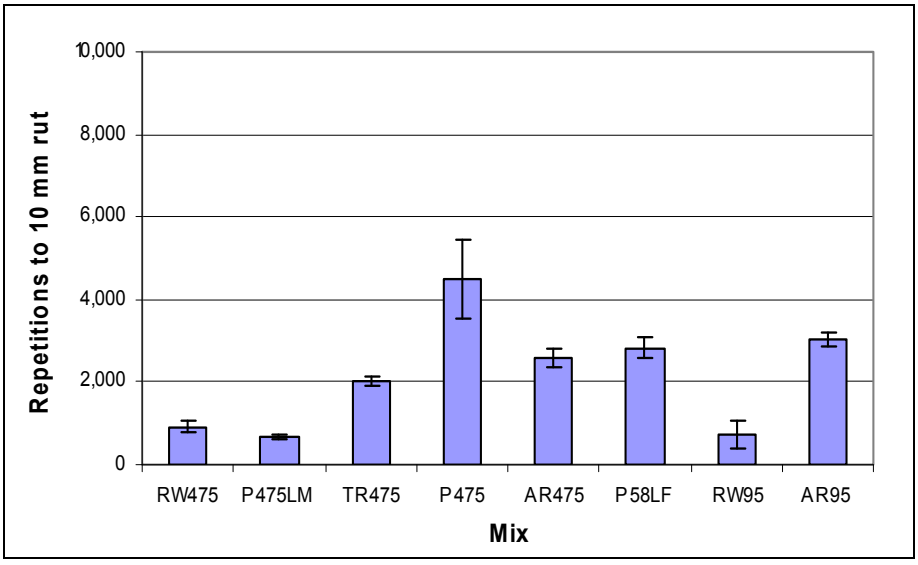

Figure 7.9: Comparison of effect of different binders on moisture sensitivity.
(Results for mixes with basalt aggregate and 4.75 mm and 9.5 mm maximum aggregate size)

Figure 7.10 shows the effects of better compaction for 4.75 mm asphalt rubber mixes with two different gradations. The results indicate that the better compaction improved the results for both gradations, despite both gradations showing similar permeabilities (see Figure 7.5).

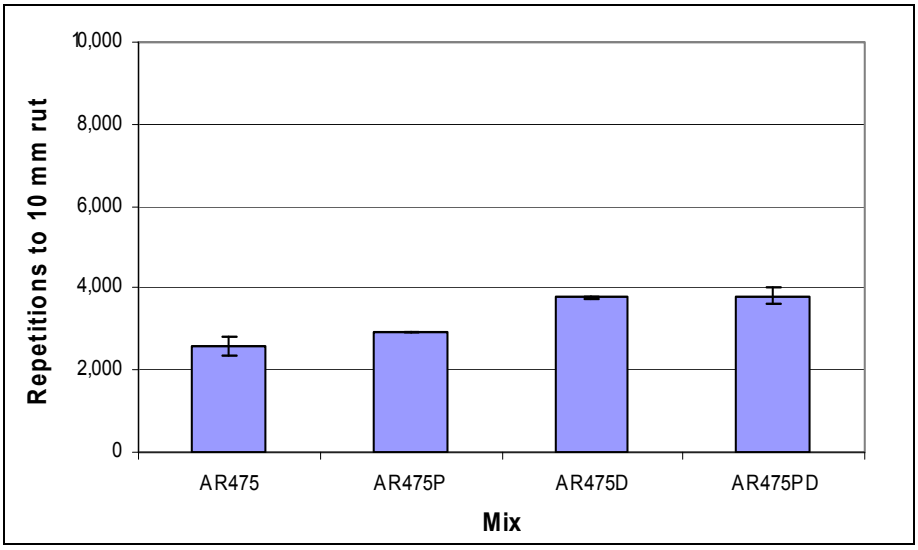

Figure 7.10: Comparison of effect of better compaction on moisture sensitivity (4.75 mm mixes).

Figure 7.11 shows the effects of different aggregate types on moisture sensitivity. There was no clear trend when the alluvial and granite aggregates were compared with mixes with basalt aggregate.

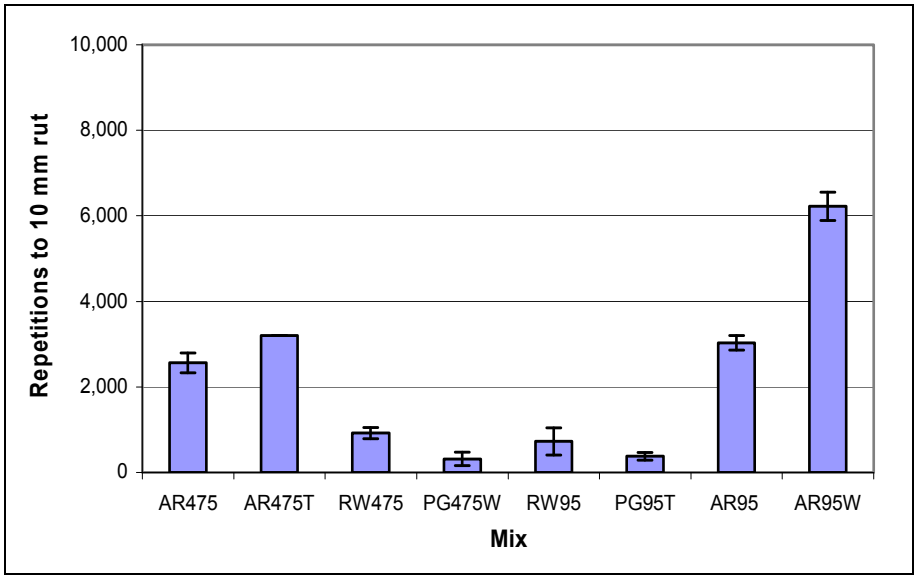

Figure 7.11: Comparison of effect of different aggregate types on moisture sensitivity.
(Results for PG64-16 and asphalt rubber mixes with 4.75 mm and 9.5 mm maximum aggregate size)

7.5.3 Rutting Resistance

Figure 7.12 shows results for all mixes tested for shear stiffness at 45°C and 0.1 second loading time. The control dense-graded mix was considerably stiffer than the open-graded mixes, as expected. Ten of the eighteen open-graded mixes had similar stiffnesses. Additional analysis is being undertaken to identify trends with respect to maximum aggregate size, gradation, and binder type and will be discussed in the final report. Generally, the courser mixes (> 12.5 mm) and some of the mixes with lime had higher stiffnesses. Fibers did not appear to have a significant influence on stiffness. Pavement thickness design will be dependent on stiffness; however, lower stiffness can be compensated for by a thicker asphalt layer, provided that the material also provides adequate rutting resistance (as indicated for example by the HWTT).

Figure 7.13 provides a comparison of the effects of maximum aggregate size on shear stiffness (45°C and 70 kPa) for mixes with basalt aggregate and PG64-16 binder. The 19 mm mix was somewhat stiffer than the mixes with smaller aggregates, but it also had more variability between replicate specimens. Stiffnesses were similar in the other three mixes, with a slight decrease in stiffness with increasing aggregate size.

Figure 7.14 provides a comparison of the effects of different binders on shear stiffness (45°C and 70 kPa) for mixes with basalt aggregate and 4.75 mm and 9.5 mm maximum aggregate size. Mixes with conventional binders appeared to have slightly higher stiffnesses than those with rubber or polymer modification.

Figure 7.15 provides a comparison of the effect of different aggregate sources (4.75 and 9.5 mm maximum aggregate size only) on shear stiffness (45°C and 70 kPa) for the mixes with PG64-16 and asphalt rubber binders. There was no clear trend in the results, although the more cubical granite aggregate tended to have a slightly higher stiffness for the same aggregate size and binder compared to the other two aggregates.

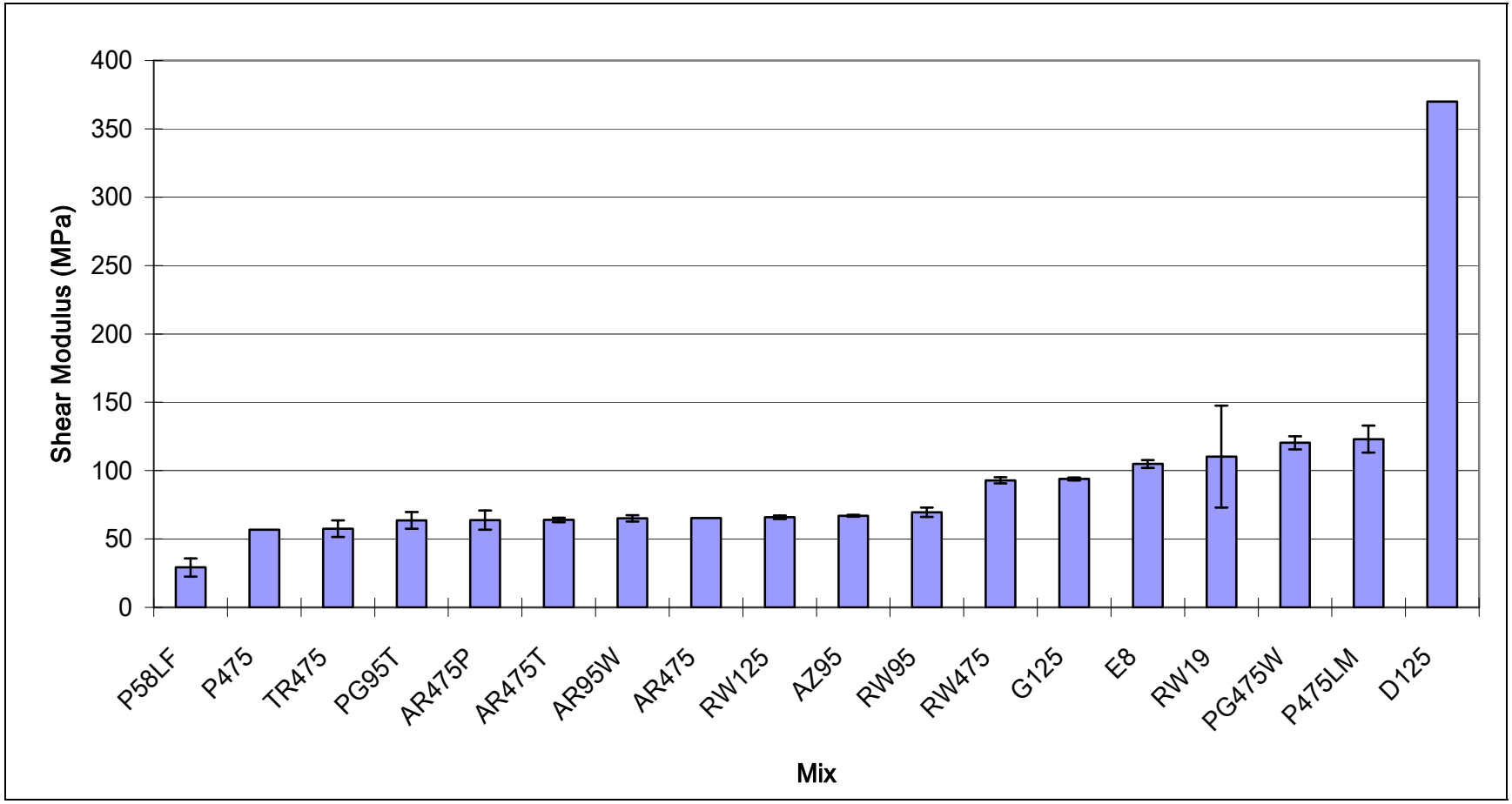

Figure 7.12: Summary plot of ranked shear stiffness (45°C & 70 kPa shear stress) results for all mixes.

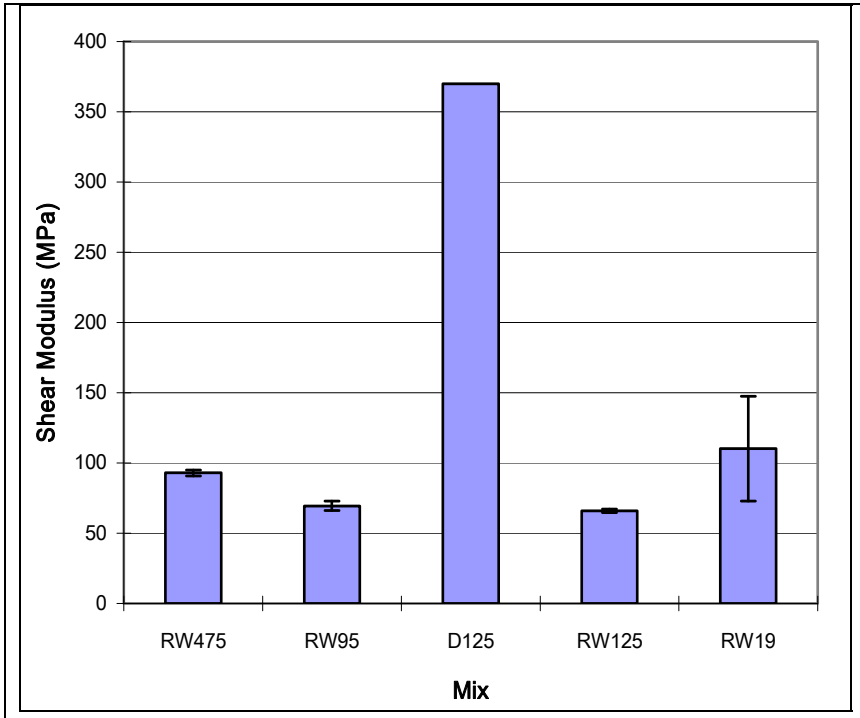

Figure 7.13: Comparison of effect of maximum aggregate size on shear stiffness.

(Results at 45°C and 70 kPa shear stress for mixes with basalt aggregate and PG64-16 binder)

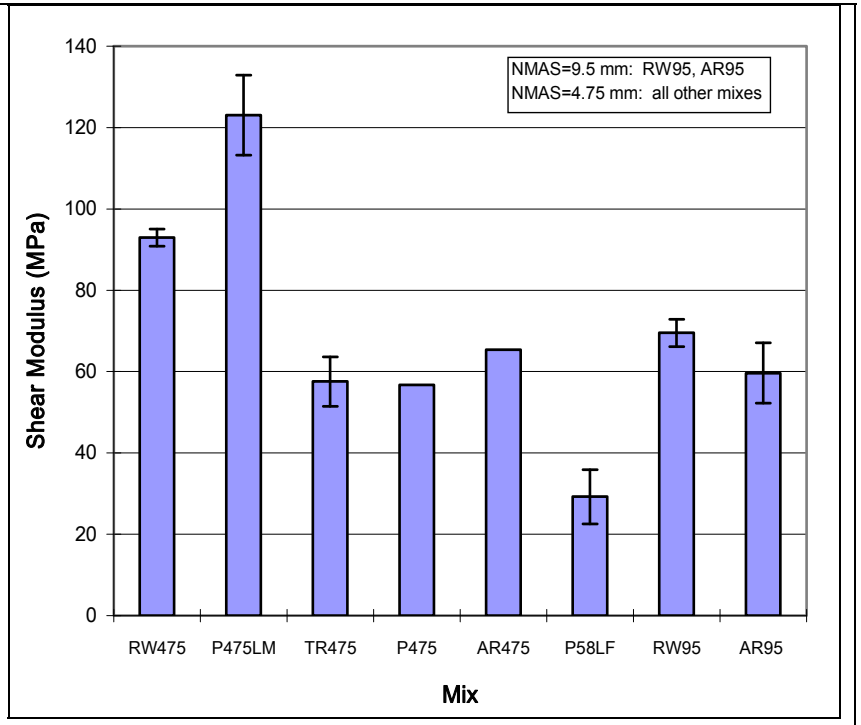

Figure 7.14: Comparison of effect of different binders on shear stiffness.

(Results at 45 C and 70 kPa shear stress for mixes with basalt aggregate and 4.75 mm and 9.5 mm maximum aggregate size)

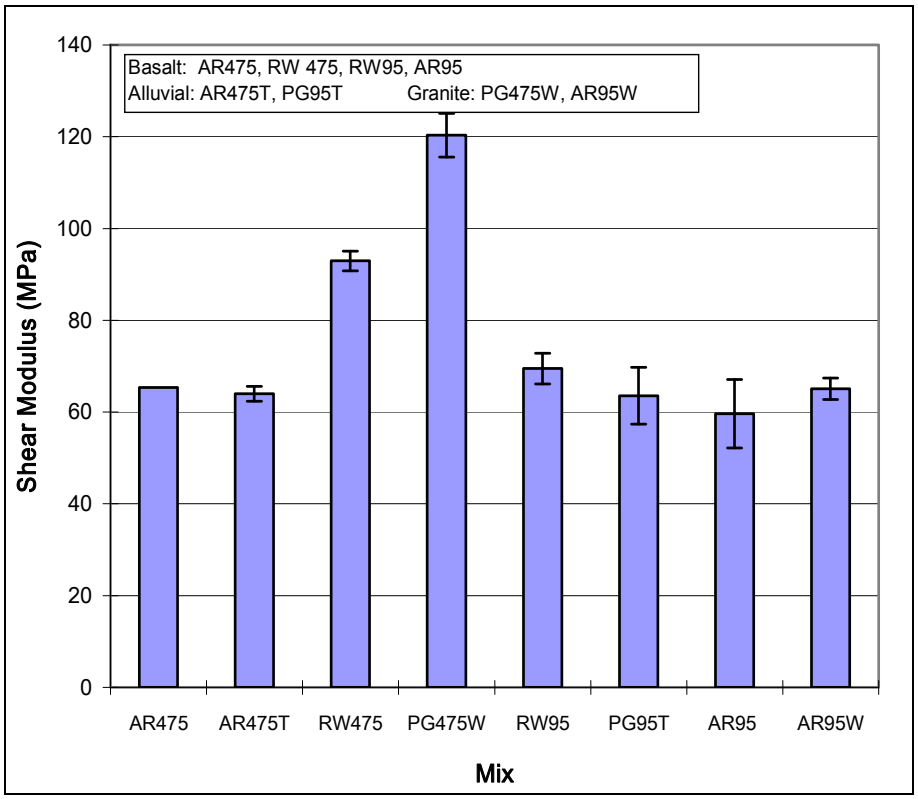

Figure 7.15: Comparison of effect of different aggregate types on shear stiffness.
(Results at 45°C and 70 kPa shear stress for mixes with PG64-16 and asphalt rubber binders and 4.75 and 9.5 mm maximum aggregate size)

7.5.4 Raveling Resistance

Raveling resistance was determined for both unaged and aged specimens, as well as for selected specimens subjected to one freeze/thaw cycle. Figure 7.16 shows the average raveling resistance for each condition. The results indicate that raveling generally increases with increasing aggregate size. Mixes with modified binders (rubberized or polymer modified) performed better than those with unmodified binders. The addition of lime and fibers also appeared to result in some improvement in performance. The 12.5 mm dense-graded control mix performed better than the open-graded 12.5 mm mixes tested, but was out-performed by the mixes with finer aggregates and modified binders.

7.5.5 Flexural Stiffness and Fatigue Cracking Resistance

At the time of preparing this report, flexural stiffness testing on the 19 mixes, and fatigue beam testing on the three mixes selected for Phase 2 testing had not been completed. The results of these tests, together with the results of fatigue testing on the European mix specimens obtained from the test track in Spain, will be discussed in the final report.

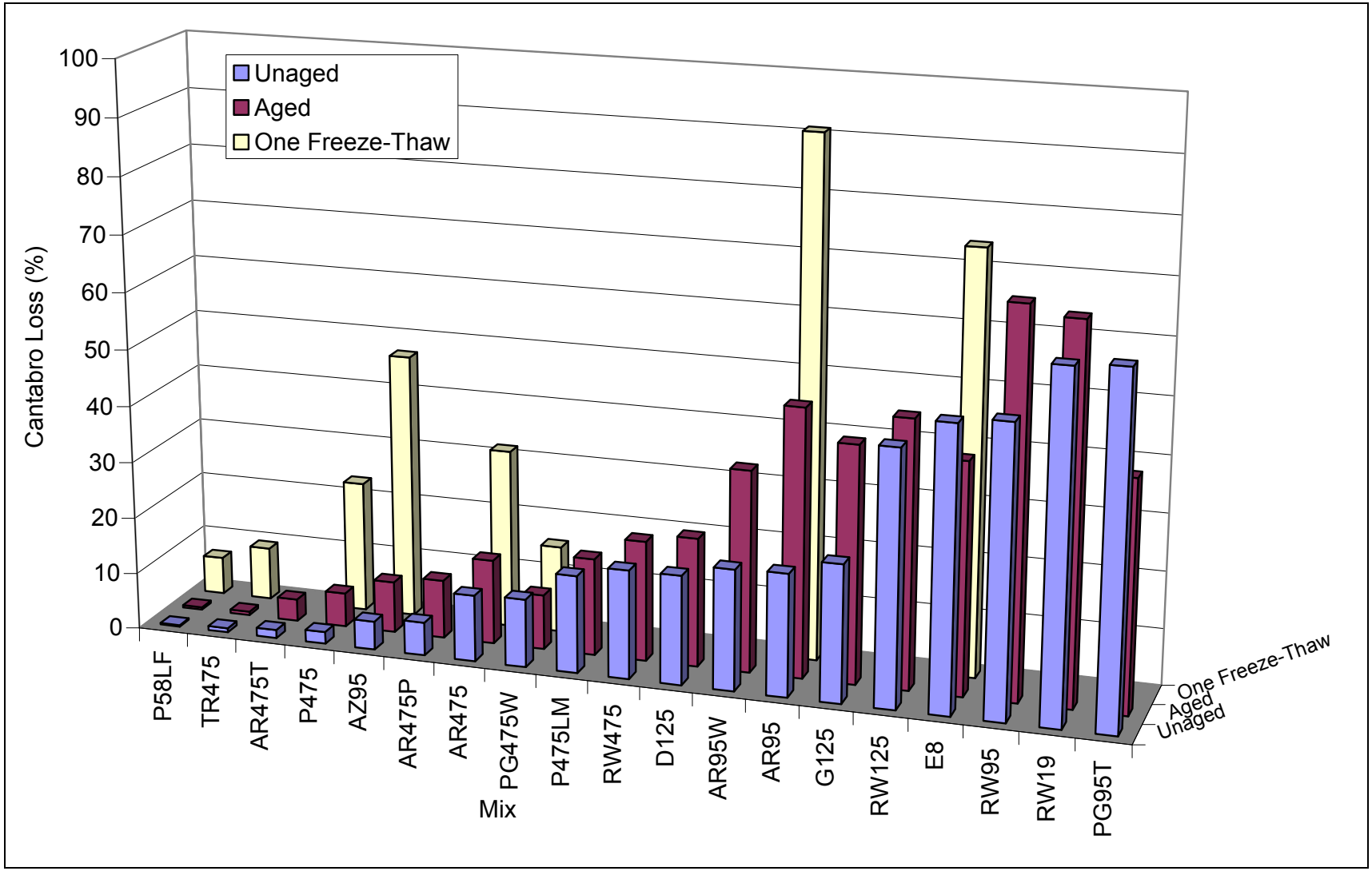

Figure 7.16: Summary plot of ranked raveling resistance results for all mixes.

7.6 Summary

Test results available to date indicate that the aggregate particle size distribution in the mix, and the binder type will be the two most critical factors in designing permeable asphalt concrete wearing courses. Sufficient permeability for anticipated needs in California was obtained on a range of mixes tested. Adequate resistance to rutting of the surface material will probably be obtained on thinner designs provided there is adequate support from underlying layers. Some moisture sensitivity was evident, but this can be overcome by the use of appropriate anti-strip mechanisms. Most of the mixes of interest had adequate durability (resistance to raveling) compared to the dense-graded control. Flexural stiffness and fatigue cracking resistance of the various mixes are still under investigation and will be discussed in the final report.

Chapter 8. Summary and Future Work

This technical memorandum summarizes the laboratory testing completed to date on a study to assess the mechanical properties of permeable pavement materials. Testing focused on subgrade and base course materials, and portland cement concrete and asphalt concrete wearing courses. Key findings include:

- The results of tests on two different subgrade soils common in the Central Valley of California indicate that both soil types will offer very little support to a pavement structure, and that the stiffness and the associated strength of the materials will decrease significantly as the moisture content increases. Any fully permeable pavement structure on these materials will need to compensate for this poor bearing capacity with thicker base and surfacing layers.
- The results of tests on four different commercially available permeable base-course aggregates indicate that these materials will probably provide sufficient support for typical traffic loads in parking lots, basic access streets and driveways, and on highway shoulders, whilst serving as a reservoir layer for the pavement structure. Although three of the four materials tested had smaller maximum aggregate sizes that those typically discussed in the literature, the permeability was still adequate for California rainfall events. The required thickness of the base and the expected structural performance in terms of the pavement structure will be discussed in a later report.
- The results from tests on portland cement concrete indicate a clear relationship between aggregate grading, cement content, water-to-cement ratio, and strength and permeability. All specimens tested exceeded the anticipated permeability requirements, indicating that aggregate gradings and cement contents can be adjusted to increase the strength of the material whilst still retaining adequate water flow through the pavement. The water-to-cement ratio appears to be critical in ensuring good constructability and subsequent performance of the pavement. Although no durability testing was carried out, the mixes are likely to have some susceptibility to raveling under traffic. Coefficient of thermal expansion of the various mixes is still under investigation and will be discussed in the final report.
- Test results available to date indicate that the aggregate particle size distribution in the mix, and the binder type will be the two most critical factors in designing permeable asphalt concrete wearing courses. Sufficient permeability for anticipated needs in California was obtained on a range of mixes tested. Adequate rutting resistance will probably be obtained on thinner designs provided there is adequate support from underlying layers. Some moisture sensitivity was evident, but this can be overcome by the use of appropriate anti-strip mechanisms. Most of the mixes of interest had adequate durability (resistance to raveling) compared to the dense-graded control. Flexural stiffness and fatigue cracking resistance of the various mixes are still under investigation and will be discussed in the final report.

Work still to be completed on this study includes the following. Findings will be documented in separate technical memorandums and in the final report. Recommendations for future work, if required, will be made in the final report on completion of all of the studies.

- Estimate pavement performance for prototype designs using the laboratory test results in pavement performance models.
- Perform a preliminary life-cycle cost analysis of the various options.
- Based on the results of the computer model analysis, develop detailed structural designs for HVS and field test sections that include pavement dimensions and material specifications.

Chapter 9. References

1. HANSEN, B. 2007. Storm-Water Management: Porous Pavement Increases Storage Area at Portland Marine Terminal. **Civil Engineering, Vol.77, No3.** Reston, VA: American Society of Civil Engineers.
2. HANSEN, K. 2008. **Porous Asphalt Pavements for Stormwater Management.** Lanham, MD: National Asphalt Pavement Association. (Information Series 131).
3. **Stormwater Management with Pervious Concrete Pavement.** 2009. Skokie, IL: American Concrete Pavement Association.
4. SMITH, D.R. 2006. **Permeable Interlocking Concrete Pavements. Selection, Design, Construction, and Maintenance.** Herndon, VA. Interlocking Concrete Pavement Institute.
5. JONES, D., Signore, J., Harvey, J.T, and Kayhanian, M. 2008. **Laboratory Testing and Modeling for Structural Performance of Permeable Pavements under Heavy Traffic.** Davis and Berkeley, CA: University of California Pavement Research Center. (Proposal and workplan prepared for Caltrans Division of Environmental Analysis).
6. TUTUMLUER, E. 1995. **Predicting Behaviour of Flexible Pavements with Granular Bases.** Atlanta, GA: Georgia Institute of Technology. (Ph.D. dissertation).
7. BEJARANO, M.O. and Thompson, M.R. 1999. **Subgrade Soil Evaluation for the Design of Airport Flexible Pavements**. University Illinois at Urbana Champaign. (Report to Federal Aviation Administration Center of Excellence for Airport Pavements. COE Report No. 8).
8. TUTUMLUER, E. and Seyhan, U. 1999. Laboratory Determination of Anisotropic Aggregate Resilient Moduli Using an Innovative Test Device. **Transportation Research Record: Journal of the Transportation Research Board.** Washington, DC: Transportation Research Board. (TRR 1687).
9. **Resilient Modulus Testing Open-Graded Drainage Layer Aggregates.** 2005. Toronto, ON: Applied Research Associates.
10. ZHANG, J., Harvey, J.T., Ali, A. and Roesler, J. 2004. **Goal 4 Long Life Pavement Rehabilitation Strategies - Rigid: Laboratory Strength, Shrinkage, and Thermal Expansion of Hydraulic Cement Concrete Mixes.** Berkeley, CA: University of California Pavement Research Center. (UCPRC-RR-2004-01).